iScience

CellPress

Article

Single-Stranded DNA-Binding Protein and Exogenous RecBCD Inhibitors Enhance Phage-Derived Homologous Recombination in *Pseudomonas*

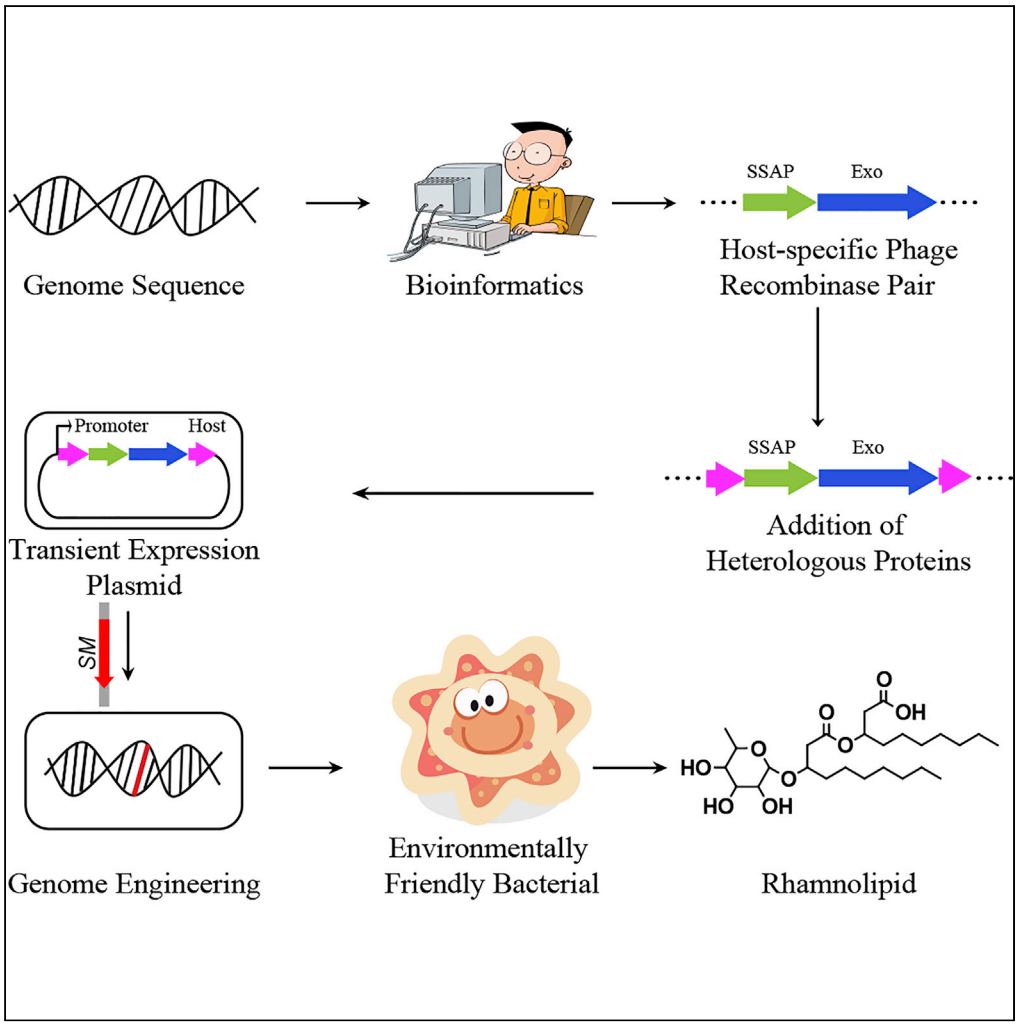

Jia Yin, Wentao Zheng, Yunsheng Gao, ..., A. Francis Stewart, Youming Zhang, Jun Fu

francis.stewart@tu-dresden.de (A.F.S.)
zhangyouming@sdu.edu.cn (Y.Z.)
fujun@sdu.edu.cn (J.F.)

HIGHLIGHTS

The BAS operon is a generic recombineering system for *Pseudomonas* species

Single-stranded DNA-binding proteins (SSBs) can stimulate homologous recombination

The heterologous gam genes can inhibit RecBCD function in *Pseudomonas*

Yin et al., iScience 14, 1–14
April 26, 2019
https://doi.org/10.1016/j.isci.2019.03.007

iScience

CellPress

Article

Single-Stranded DNA-Binding Protein and Exogenous RecBCD Inhibitors Enhance Phage-Derived Homologous Recombination in *Pseudomonas*

Jia Yin,[1,2,5] Wentao Zheng,[1,5] Yunsheng Gao,[1] Chanjuan Jiang,[1] Hongbo Shi,[1] Xiaotong Diao,[1] Shanshan Li,[1] Hanna Chen,[2] Hailong Wang,[1] Ruijuan Li,[1] Aiying Li,[1] Liqiu Xia,[2] Yulong Yin,[2,3] A. Francis Stewart,[4,*] Youming Zhang,[1,*] and Jun Fu[1,6,*]

SUMMARY

The limited efficiency of the available tools for genetic manipulation of *Pseudomonas* limits fundamental research and utilization of this genus. We explored the properties of a *lambda* Red-like operon (BAS) from *Pseudomonas aeruginosa* phage Ab31 and a Rac bacteriophage RecET-like operon (RecTE$_{Psy}$) from *Pseudomonas syringae* pv. syringae B728a. Compared with RecTE$_{Psy}$, the BAS operon was functional at a higher temperature indicating potential to be a generic system for *Pseudomonas*. Owing to the lack of RecBCD inhibitor in the BAS operon, we added Redγ or Pluγ and found increased recombineering efficiencies in *P. aeruginosa* and *Pseudomonas fluorescens* but not in *Pseudomonas putida* and *P. syringae*. Overexpression of single-stranded DNA-binding protein enhanced recombineering in several contexts including RecET recombination in *E. coli*. The utility of these systems was demonstrated by engineering *P. aeruginosa* genomes to create an attenuated rhamnolipid producer. Our work enhances the potential for functional genomics in *Pseudomonas*.

INTRODUCTION

Recombinant DNA technology in *Escherichia coli* (*E. coli*) has been greatly boosted by bacteriophage-encoded recombination systems (Muyrers et al., 1999; Zhang et al., 1998, 2000). A decisive advantage of this technology, termed recombinogenic engineering or recombineering, is the easy incorporation of the flanking short homology sequences required for homologous recombination into synthetic oligonucleotides. Oligonucleotides and linear dsDNAs with homology arms as short as 35 nucleotides have been exploited in many ways for point mutations, deletions, insertions, and subcloning with base pair precision regardless of the size of the target DNA (Murphy, 1998; Muyrers et al., 1999; Zhang et al., 1998, 2000).

In *E. coli*, recombineering utilizes the Redα, Redβ, and Redγ proteins from the *lambda* phage Red operon or RecE and RecT from the Rac prophage (Fu et al., 2012; Zhang et al., 1998). Redα and RecE are 5′-3′ exonucleases that generate single-stranded DNA (ssDNA) intermediates (Maresca et al., 2010). Redβ and RecT are single-stranded DNA-annealing proteins (SSAPs) that bind to ssDNA to promote the search for the complementary sequence (Erler et al., 2009). The Redα/Redβ and RecE/RecT phage pairs each include a specific protein-protein interaction, which is required for double-stranded DNA (dsDNA) homologous recombination (Muyrers et al., 2000).

Redγ forms a dimer to mimic DNA that binds to and inhibits the exonuclease and helicase activities of the RecBCD complex (Court et al., 2007; Murphy, 1991), which aggressively degrades linear dsDNA (Court et al., 2007; Wang et al., 2006). The RecET operon does not appear to have a Redγ equivalent. However, the inclusion of Redγ with RecE/RecT increases homologous recombination efficiency via increased persistence of the linear dsDNA substrates (Fu et al., 2012; Zhang et al., 1998). The significance of a RecBCD inhibitor for homologous recombination efficiency was also demonstrated in our study describing *Photorhabdus luminescens* Pluγ for the development of a recombineering system for *Photorhabdus* and *Xenorhabdus*. We found that Pluγ could inhibit the RecBCD complex in both *Photorhabdus* and *E. coli* (Yin et al., 2015).

The Red system has been applied to precisely and fluently edit the genome of not only *E. coli* but also closely related bacteria *Salmonella enterica* (Bunny et al., 2002), *Yersinia pseudotuberculosis* (Derbise

[1]Shandong University-Helmholtz Institute of Biotechnology, State Key Laboratory of Microbial Technology, Suzhou Institute of Shandong University, 266235 Qingdao, China

[2]Hunan International Joint Laboratory of Animal Intestinal Ecology and Health, Laboratory of Animal Nutrition and Human Health, College of Life Sciences, Hunan Normal University, 410081 Changsha, China

[3]Chinese Academy of Science, Institute of Subtropical Agriculture, Research Center for Healthy Breeding of Livestock and Poultry, Hunan Engineering and Research Center of Animal and Poultry Science and Key Laboratory for Agroecological Processes in Subtropical Region, Scientific Observation and Experimental Station of Animal Nutrition and Feed Science in South-Central, Ministry of Agriculture, 410125 Changsha, China

[4]Biotechnology Research Center, Center for Molecular and Cellular Bioengineering, Dresden University of Technology, BioInnovationsZentrum, Tatzberg 47-51, 01307 Dresden, Germany

[5]The authors contributed equally

[6]Lead Contact

*Correspondence: francis.stewart@tu-dresden.de (A.F.S.), zhangyouming@sdu.edu.cn (Y.Z.), fujun@sdu.edu.cn (J.F.)

https://doi.org/10.1016/j.isci.2019.03.007

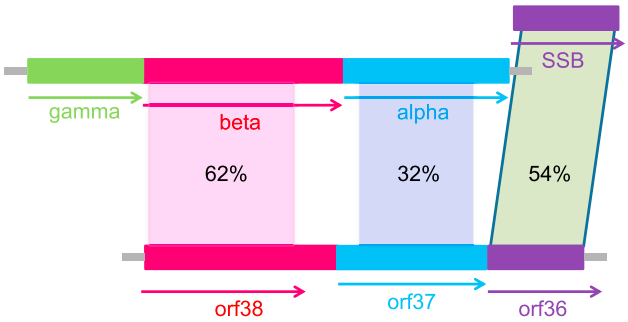

Figure 1. Operon Architecture of Lambda Red and *Pseudomonas* Phage vB_PaeP_Tr60_Ab31 orf36-orf38 Orf38, Orf37, and Orf36 Are Related to Redβ (beta), Redα (alpha), and SSB, Respectively

The amino acid sequences were compared via ClustalW alignment (Figure S1). The percent identities are displayed between the homology regions.

et al., 2003), *Shigella* (Beloin et al., 2003), *Serratia* (Rossi et al., 2003), and *Escherichia albertii* (Egan et al., 2016). However, its wider application has been limited by apparent host specificities (Yin et al., 2015). Consequently endogenous SSAPs alone or together with partner exonucleases have been used for oligo repair or cassette insertion in *Mycobacterium tuberculosis* (Van Kessel and Hatfull, 2006), *Lactococcus lactis* (Pijkeren and Britton, 2012), *Lactococcus reuteri* (Pijkeren et al., 2012), *Clostridium acetobutylicum* (Dong et al., 2013), *Lactobacillus plantarum* (Yang et al., 2015), *Bacillus subtilis* (Sun et al., 2015), *P. luminescens*, and *Xenorhabdus stockiae* (Yin et al., 2015).

Pseudomonas is a gram-negative, aerobic rod that belongs to the bacterial family Pseudomonadaceae (EUZéBY, 1997). The best characterized species include the opportunistic human pathogen *Pseudomonas aeruginosa* (Stover et al., 2000), the plant pathogen *Pseudomonas syringae* (Xin and He, 2013), the plant growth-promoting *Pseudomonas fluorescens* (Paulsen et al., 2005), and the soil bacterium *Pseudomonas putida*, which is used in bioremediation (Gomes et al., 2005) and biocontrol (Validov et al., 2007). The members of this genus demonstrate a great deal of metabolic diversity (Aditi et al., 2017).

Here, we report the development of recombineering systems for *Pseudomonas* based on two host-specific phage protein-encoding operons from *P. aeruginosa* phage Ab31 and *P. syringae*. BLAST analysis suggested that Orf38, Orf37, and Orf36 are analogs of Redβ, Redα, and single-stranded DNA-binding protein (SSB), respectively. Recombineering experiments indicated that Redγ or Pluγ worked in some *Pseudomonas* species and SSB significantly increased efficiency. SSBs are often found in recombinase-encoding operons from various phages (Szczepańska, 2009). Because proteins in the same operon are usually functionally associated, we were particularly interested in evaluating the contribution of orf36/S to phage recombinase-mediated homologous recombination. Using these systems, we efficiently modified *Pseudomonas* genomes including gene deletions and insertions. In particular, a highly attenuated rhamnolipid producer was obtained after deleting pathogenic factors and overexpressing *rhl*AB and *est*A in *P. aeruginosa*.

RESULTS

Endogenous Phage exo/SSAP Protein Pairs in *Pseudomonas*

We looked for candidate DNA recombination proteins in *Pseudomonas* and *Pseudomonas* phage genomes with BLAST using the coding sequences of λ Redβ, *rac* RecT, or Pluβ as queries in a non-redundant protein sequence database. Two operons including an exonuclease (exo) and SSAP were identified. One was $RecTE_{Psy}$ from *P. syringae*, which was previously developed as a recombineering system for use in *P. syringae* (Swingle et al., 2010). The second operon, from *P. aeruginosa* phage vB_PaeP_Tr60_Ab31, encoded three proteins including a candidate SSAP (orf38, here named *B*) that was 62% identical to Redβ over its 177-amino acid sequence (Figure 1) and was adjacent to a candidate exonuclease (orf37, here named *A*; Figure 1), which showed significant similarity to Redα (sequence identity of 32% in a 195-amino acid region). The next coding region, orf36 (here named *S*), showed significant similarity to SSBs (sequence identity of 54% across 148 amino acids of the *E. coli* SSB; Figure 1). SSBs are often found

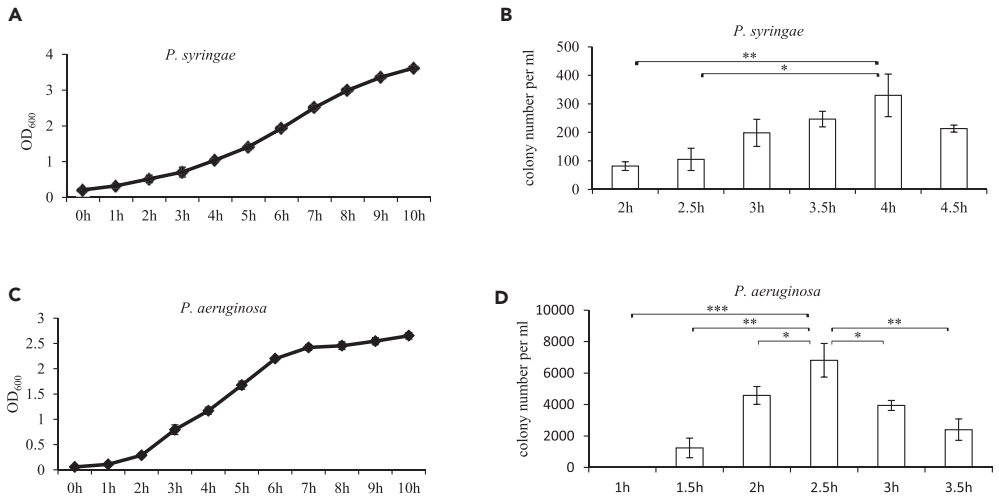

Figure 2. Optimization of Transformation in *P. syringeae* and *P. aeruginosa*

(A) Growth curve of *P. syringeae*. The optical density (OD) at 600 nm (OD_{600}) was measured from a starting OD_{600} of 0.085.

(B) Time when cells were harvested for electroporation.

(C and D) (C) and (D) are the same as (A) and (B), respectively, for *P. aeruginosa*. After electroporation of pBBR1-rha-GFP-km, colonies were selected on kanamycin plates and counted.

Data represent the mean ± SD from three independent experiments. The statistical analysis used is Student's t test. *p < 0.05, **p < 0.01, ***p < 0.001.

in recombinase-encoding operons from various phages (Szczepańska, 2009). Because proteins in the same operon are usually functionally associated, we evaluated the contribution of orf36/S to phage recombinase-mediated homologous recombination and we named this candidate recombineering operon, *BAS*.

In gram-negative bacteria, RecBCD, which is the major exonuclease in *E. coli*, is highly conserved (Table S5). Notably neither $RecTE_{Psy}$ nor BAS operons contained a homolog of Redγ or Pluγ, which are inhibitors of RecBCD exonuclease activity. Because co-expression of Redγ with Redβα or RecET significantly increases recombineering efficiency (Fu et al., 2012), the addition of Redγ or Pluγ to the $RecTE_{Psy}$ and BAS operons were tested for their abilities to increase recombineering efficiency.

Critical Time Points for Electroporation of *Pseudomonas*

In *E. coli*, transformation efficiency determines optimal recombineering (Sharan et al., 2009). When *E. coli* DH10B-derived cells are used, the recombinant proteins are usually induced when the cells enter log phase growth (OD_{600} = 0.30–0.35). After two cell divisions, at OD_{600} = 0.70–0.80, the electrocompetent cells are prepared (Fu et al., 2010). This principle was also verified by recombineering in *Photorhabdus* (Yin et al., 2015). To optimize protocols for *Pseudomonas*, we first plotted the growth of the four *Pseudomonas* strains at 30°C. Overnight cultures were diluted to $OD_{600} \approx 0.085$ to start the growth-monitoring cultures. After approximately 2 h, *P. syringae* and *P. aeruginosa* cultures entered the log phase and the plasmid pBBR1-Rha-GFP-kan was transformed into electrocompetent cells prepared at different time points (Figure 2). We found that cells prepared at 4 and 2.5 h, respectively, yielded the most transformants (Figures 2B and 2D). The same test was performed for *P. fluorescens* (Figures S2A and S2B) and *P. putida* (Figures S2C and S2D). Thereby we established the time points for induction and electrocompetent preparation for each strain (Table S6).

Efficiency of Recombineering Systems in *Pseudomonas*

We compared the $RecTE_{Psy}$, BAS, Redγβα, and Pluγβα systems in four *Pseudomonas* strains. Pluγ or Redγ was added to the $RecTE_{Psy}$ and BAS operons to generate four more candidate systems: $PluγTE_{Psy}$, $RedγTE_{Psy}$, PluγBAS, and RedγBAS. The eight expression plasmids were transformed into the four *Pseudomonas* strains, followed by plasmid DNA extraction and restriction analysis for confirmation. The expression plasmids were based on a broad host range origin (pBBR1) (Antoine and Locht, 1992), and

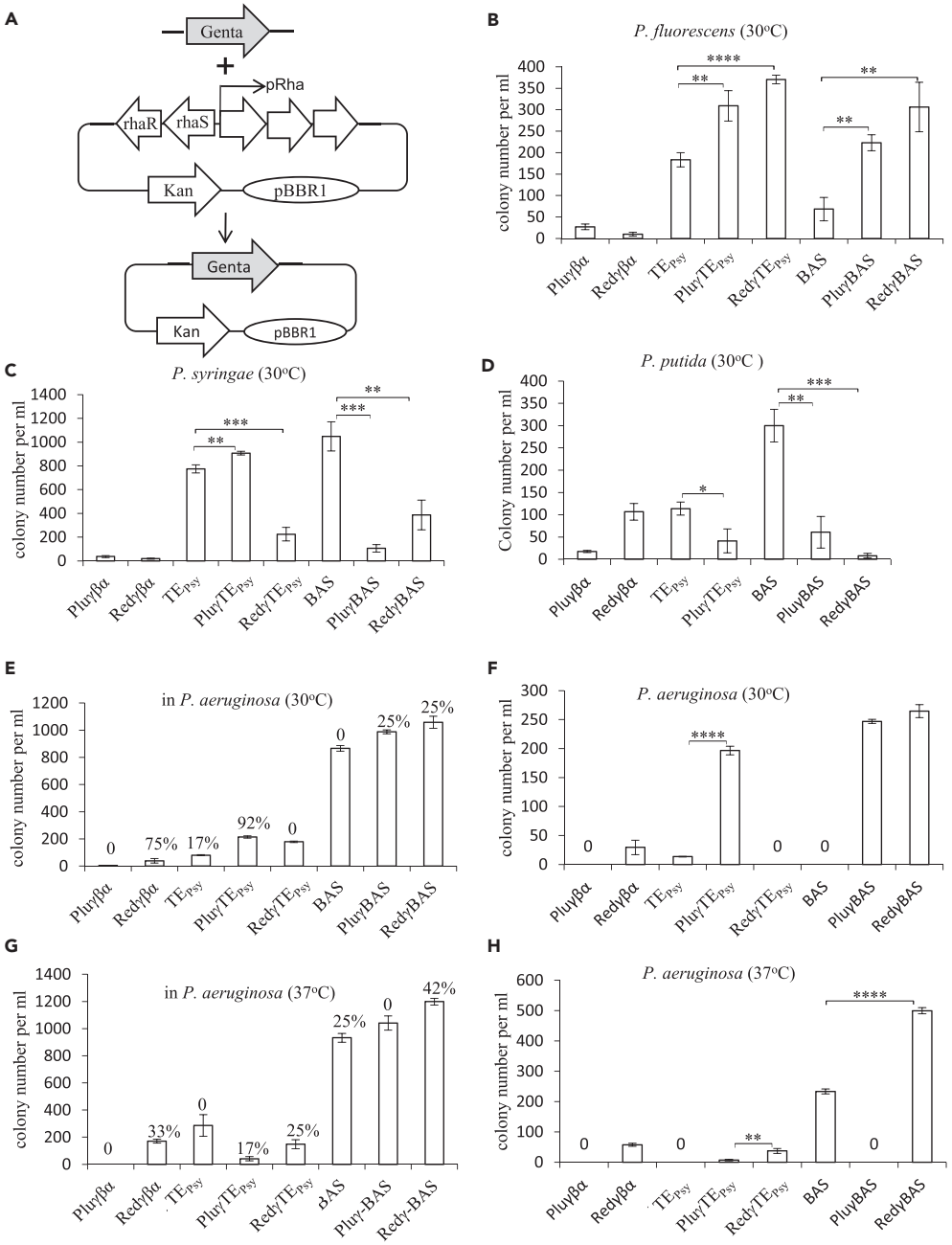

Figure 3. Recombineering with Different Protein Combinations in Different *Pseudomonas* Species

(A) Diagram of the recombineering assay. A PCR product carrying a gentamycin resistance gene (Genta) flanked by 100-bp homology arms (thick lines) was integrated into the expression plasmid in place of the artificial operon of the recombination system.

(B) Results from the recombineering assay in *P. fluorescens* upon the expression of Pluγβα, Redγβα, TE_{Psy}, PluγTE_{Psy}, RedγTE_{Psy}, BAS, PluγBAS, and RedγBAS at 30°C.

(C) Results from *P. syringae*, which was set up as described in (B).

(D) Results from *P. putida*, which was set up as described in (B), with the exception that RedγTE_{Psy} was missing owing to the failure of transformation.

(E) Results from *P. aeruginosa* at 30°C, which was set up as described in (B), and the correct rates are indicated at the top of each column.

(F) Results from *P. aeruginosa* at 30°C, which was calculated from the correct rates of (E), and the y axis represents the number of correct colony.

Figure 3. *Continued*

(G and H) (G) and (H) are as in (E) and (F), respectively, except the proteins were expressed at 37°C. Colonies were selected on gentamycin plates and counted.

Data represent the mean ± SD from three independent experiments. The statistical analysis used is Student's t test. *p < 0.05, **p < 0.01, ***p < 0.001, ****p < 0.0001.

the *rha*R-*rha*S P_{Rha} promoter (Egan and Schleif, 1993, 1994) was used for inducible expression of the recombination operons.

To compare the recombineering efficiency of different systems in one species, all the electroporation was carried out using competent cells prepared from a 1.3 mL fresh culture that are adjusted to the same cell density. After electroporation, 1 mL Luria-Bertani (LB) medium was added for recovery. The data presented are exactly the result from one electroporation, and this methodology was utilized in our previous study (Fu et al., 2012; Yin et al., 2015).

We used an assay based on the integration of a PCR product containing gentamycin resistance gene flanked by 100 bp homology arms into the pBBR1 expression plasmid to obtain the plasmid product, pBBR1-Kan-Genta (Figure 3A). Results are based on counting gentamycin-resistant colonies followed by verification of pBBR1-Kan-Genta by restriction analysis.

P. fluorescens, *P. syringae, and P. putida* were grown and tested at 30°C (Figures 3B–3D). Eight recombinants of pBBR1-Kan-Genta were verified by restriction analysis and found to be 100% in all three strains. Expression of Pluγ and Redγ enhanced recombination in *P. fluorescens* but appeared to impair it in *P. putida* possibly because the expression of Pluγ or Redγ had a toxic effect. Indeed, we could not cultivate *P. putida* carrying the RedγTE_{Psy} expression plasmid. In all three strains, both TE_{Psy} and BAS systems worked better than Redγβα and Pluγβα.

A different outcome was observed in *P. aeruginosa* where the acquisition of gentamycin resistance, possibly due to intrinsic multidrug resistance mechanisms (Savoia, 2014), did not faithfully reflect recombination into pBBR1. Consequently, both gentamycin-resistant colonies and the correct recombination rates are presented in Figures 3E–3H. Because *P. aeruginosa* normally grows at 37°C, we tested recombination at both 30°C and 37°C. At 30°C, Pluγ significantly increased the efficiency of both the TE_{Psy} and BAS systems, but it failed to have an effect at 37°C indicating thermolability. In contrast, Redγ increased the efficiency of BAS at both 30°C and 37°C. As with the other three strains, the PluγTE_{Psy}, PluγBAS, and RedγBAS systems were superior to Redγβα and Pluγβα. Notably, the correct ratio of PluγTE_{Psy} at 30°C was 92%, which was the most efficient of all variations tested in *P. aeruginosa*. However, PluγTE_{Psy} showed no activity at 37°C and RedγBAS presented the best performance (Figures 3E–3H). We suggest that Pluγ and TE_{Psy} are inactive above 30°C and Redγ and BAS are active at 37°C. These temperature optima concord with the origins of these proteins.

Functional Dissection of BAS

Based on the above evaluation, the BAS system, with or without Redγ, can be used for genome engineering in various *Pseudomonas* strains. Because the single-stranded DNA-binding protein S is the unusual aspect of this operon, we further investigated its contribution to recombineering first in *E. coli* where neither BA nor BAS functioned well without Redγ. However, in the presence of Redγ, S promoted recombineering efficiency about 4-fold (Figure 4A). A similar effect was found in *P. aeruginosa* (Figure 4B), whereas in *P. syringae*, Redγ stimulated recombination in the absence of S but impaired it in its presence (Figure 4C).

To further investigate the effect of S, we evaluated its effect of Red- and RecET-mediated recombination, which differ mechanistically. Redγβα requires a replicating substrate and acts at the replication fork (Maresca et al., 2010), whereas full-length RecE/RecT recombines two linear DNAs before replication (Fu et al., 2012). We term these two mechanisms linear plus circular homologous recombination (LCHR) and linear plus linear homologous recombination (LLHR). Addition of S to Red LCHR has a small positive effect, whereas it substantially enhances RecET LCHR (Figure 4D). Conversely, S does not convey LLHR capacity onto Red but substantially enhances RecET LLHR (Figure 4E). Consequently, we tried two more SSBs, which are from *E. coli* and F plasmid, and both also enhanced RecET LLHR (Figure 4F).

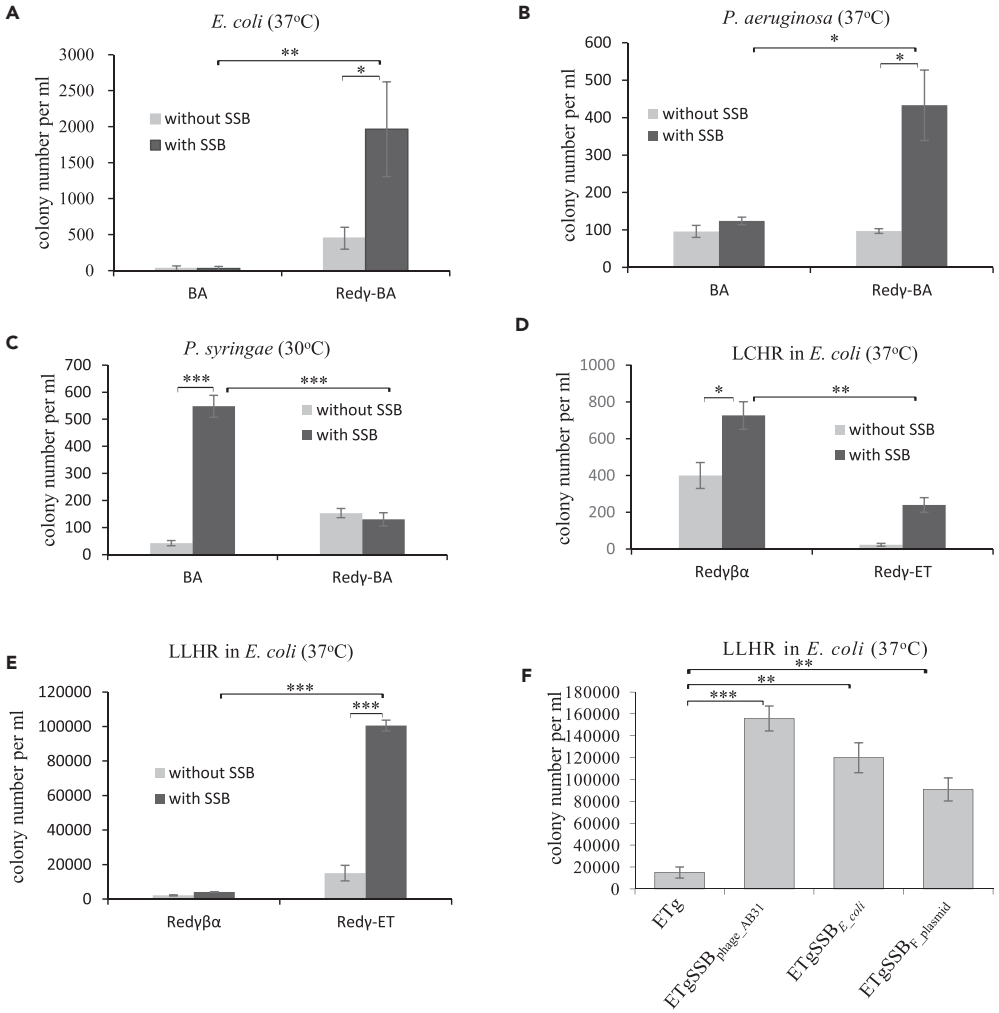

Figure 4. Functional Analysis of SSB

(A–C) Results from the recombineering assay in Figure 3A in *E. coli*, (A), *P. aeruginosa* (B), and *P. syringae* (C) upon expression of BA or RedγBA in the presence and absence of SSB. Colonies were selected on gentamycin plates and counted.

(D) Results from LCHR assay in *E. coli* upon expression of RedγBA or RecET-Redγ in the presence and absence of SSB.

(E) As in (D) except using LCHR assay.

(F) Efficiency of LLHR mediated by ETg, $ETgSSB_{phage\_Ab31}$, $ETgSSB_{E\_coli}$, and $ETgSSB_{F\_plasmid}$. Colonies were selected on chloramphenicol or kanamycin plates and counted.

Data represent the mean ± SD from three independent experiments. The statistical analysis used is Student's t test. *p < 0.05, **p < 0.001, ***p < 0.0001.

Optimization of Recombineering in *Pseudomonas*

After identifying the optimal recombineering configurations for each *Pseudomonas* strain, i.e., $PluγTE_{Psy}$ for *P. aeruginosa* at 30°C, RedγBAS for *P. aeruginosa* at 37°C, BAS for *P. putida* and *P. syringae*, and $RedγTE_{Psy}$ or RedγBAS for *P. fluorescens*, we further optimized the protocols. Apart from electrocompetent cell preparation, the amount of DNA to be transformed and the length of its homology arm to the target play large roles in determining efficiency (Fu et al., 2012; Yin et al., 2015). We titrated the DNA amount from 100 ng to 2 μg. It was observed that 1 μg DNA was sufficient for *P. fluorescens*, *P. syringae*, and *P. putida* (Figures S3A, S3C, and S3E). However, *P. aeruginosa* required 1.5 μg of DNA to achieve a decent efficiency (Figure S3G). For all three strains, the saturation amount of DNA was 1.5 μg. The length of the homology arm was tested across a range from 30 to 150 bp. One hundred base pairs were sufficient for *P. fluorescens* (Figure S3B) and *P. putida* (Figure S3F). *P. syringae* (Figure S3D) and *P. aeruginosa*

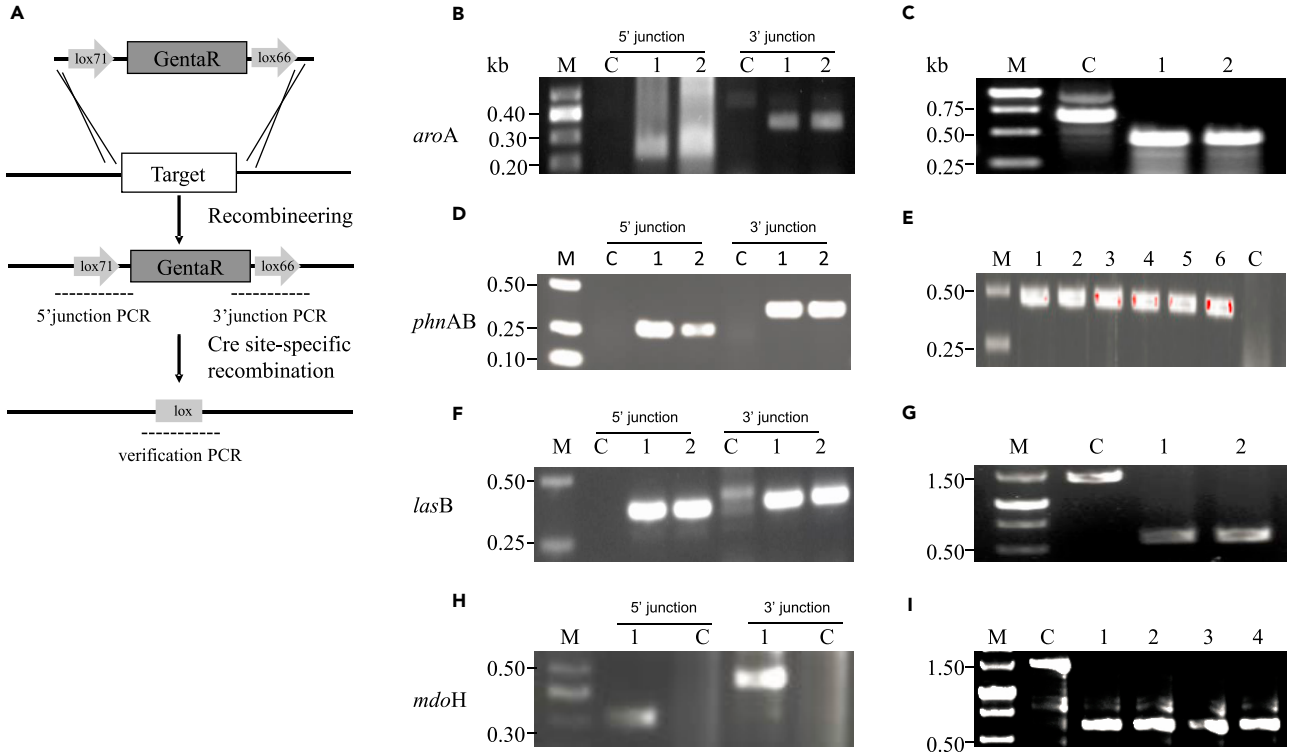

Figure 5. PCR Verification of the Genome Engineering of *P. aeruginosa* by Recombineering through RedγBAS System at 37°C

(A) Diagram of the genome engineering of *P. aeruginosa* and schematic presentation of the PCR setup for verification.

(B) *aro*A gene knockout via replacement with a gentamycin selection marker. Lane C is the wild-type strain, used as a negative control. Lane M is the Takara DL5000 marker. Lanes 1 and 2 are recombinants. Both clones 1 and 2 are correct.

(C) Gentamycin selection marker deletion via Cre recombination for *aro*A gene knockout. Both clones 1 and 2 are correct.

(D) *phn*AB gene knockout via replacement with a gentamycin selection marker. Both clones 1 and 2 are correct.

(E) Gentamycin selection marker deletion via Cre recombination for *phn*AB gene knockout. Six clones are correct.

(F) *las*B gene knockout via replacement with a gentamycin selection marker. Both clones 1 and 2 are correct.

(G) Gentamycin selection marker deletion via Cre recombination after *las*B gene knockout. Both clones are correct.

(H) *mdo*H gene knockout via replacement with a gentamycin selection marker. The tested clone is correct.

(I) Gentamycin selection marker deletion via Cre recombination after *mdo*H gene knockout. Four clones are correct.

(Figure S3H) required 120 bp for significantly higher efficiency. Although a 150-bp homology arm further boosted the efficiency for *P. aeruginosa*, we did not employ this advantage owing to cost and concerns over the quality of long oligonucleotide syntheses.

Recombineering *Pseudomonas* Genomes

To validate the methods, we designed several genome engineering exercises beginning with the construction of an attenuated *P. aeruginosa* PAO1 mutant. *P. aeruginosa* produces a number of virulence factors, including exotoxin A (McEwan et al., 2012), pyocyanin (Yang et al., 2016), elastase (McIver et al., 1991), and periplasmic glucans (Mahajan-Miklos et al., 1999), which prevent the safe use of this strain for the production of rhamnolipids. As diagrammed in Figure 5A, a number of gene knockouts were performed by electroporating a PCR product containing a gentamycin resistance gene flanked by lox71/lox66 sites and 75-bp homology arms. The *aro*A gene (1917 bp) encodes 3-phosphoshikimate 1-carboxyvinyltransferase, which is essential for the synthesis of aromatic amino acids. Deletion of *aro*A can completely prevent *P. aeruginosa* infection of mammalian cells (Priebe et al., 2002). The *phn*AB (2172bp) gene is involved in pyocyanin biosynthesis (Lau et al., 2004). The *las*B gene (1497 bp) encodes elastase (McIver et al., 1991). The *mdo*H gene (2586 bp) is required for the biosynthesis of periplasmic glucans (Mahajan-Miklos et al., 1999). To knock out these genes, each electroporation yielded approximately 100 gentamycin-resistant colonies when PluγTE$_{Psy}$ was expressed, and all the clones were correct. We also used the RedγBAS system and noticed approximately 1000 small and 100 large gentamycin-resistant colonies, but only about half of

the large colonies were correct according to colony PCR (Figures 5B, 5D, 5F, and 5H). To generate a selectable marker-free *P. aeruginosa* PAO1 mutant, Cre catalyzed the excision of the lox-flanked DNA (Figures 5C, 5E, 5G, and 5I).

Pseudomonas exotoxin A is a single-chain toxin with three structural domains that inhibit protein synthesis in eukaryotic cells by catalyzing ADP ribosylation of elongation factor 2. The amino-terminal domain I is involved in eukaryotic cell recognition (Jinno et al., 1988), the central domain II may be involved in the translocation function of the protein (Siegall et al., 1989), and the carboxy-terminal domain III has a cleft that is proposed to be the enzyme active site (Carroll and Collier, 1987). Glu-578 in domain III has been identified as an active site residue for nicotinamide adenine dinucleotide binding (Carroll and Collier, 1987). To evaluate the ability of the recombineering system to achieve a seamless mutation, we aimed to mutate this residue. A single-nucleotide substitution of ToxA (GAG Glu-578 codon to GAC Asp) was achieved by two rounds of recombineering (Figure S4A). First, a PCR product with a gentamycin resistance and counter-selection (SacB) genes flanked by 75-bp homology arms was introduced into *P. aeruginosa* expressing PluγTE$_{Psy}$. After the gentamycin-resistant clones were verified by colony PCR (Figure S4B), SacB function was tested (Figure S5). In the second round of recombineering, a point mutation (GAG Glu-578 codon to GAC Asp) was introduced using 121-bp oligonucleotide with 60-bp homology arms either side of the point mutation. The reaction was mediated by PluγTE$_{Psy}$, and the mutant strain was screened on LB plates containing 10% sucrose. Successful site-directed mutagenesis was confirmed by colony PCR (Figure S4C) and sequencing (Figure S4D).

The BAS system was also successfully applied to genome engineering of *P. syringae* pv. tomato str. DC3000 by placing a promoter (P$_{genta}$) in front of a silent gene cluster for a secondary metabolite pathway. Insertion of the promoter was efficient. Each electroporation yielded about 120 gentamicin-resistant colonies. Three colonies were verified by colony PCR (Figure S6A), and all of them were correct. However, we could not detect any new compound produced by the engineered strain (data not shown). We also engineered the *P. fluorescens* genome with the RedγTE$_{Psy}$ system. The *ret*S gene of *P. fluorescens* was knocked out, and the mutant strain was confirmed by colony PCR (Figure S6B). Each electroporation yielded approximately 20 gentamicin-resistant colonies, and all of them were correct. The hybrid sensor kinase (RetS) negatively controls the production of antibiotics, including 2,4-diacetylphloroglucinol, pyrrolnitrin, and pyoluteorin, in *P. fluorescens* (Zhang et al., 2015). Genetic inactivation of *ret*S results in enhanced biocontrol capacity of the strain (Zhang et al., 2015).

Using the Attenuated *P. aeruginosa* PAO1 Mutant for Rhamnolipid Production

Although much effort has been invested in heterologous expression of *rhl*AB, the pathogenic strain *P. aeruginosa* PAO1 remains the best producer of rhamnolipids (Zhao et al., 2015). To evaluate the safety of an attenuated *P. aeruginosa* PAO1 strain, we examined their virulence in mice and *C. elegans* models. The 50% lethal dose for wild-type PAO1 given by intraperitoneal (i.p.) injection was 4×10^8 colony-forming unit (CFU). However, no toxic effects were observed with i.p. doses of the attenuated mutant PAO1*aro*A up to 1×10^9 CFU (Figure 6A). In contrast, the PABMT mutant (*phn*AB$^-$, *las*B$^-$, *mdo*H$^-$, and *tox*A$^-$) was still pathogenic to BALB/c mice (Table S7) and postponed the egg stage in *C. elegans* (Figure S7).

The PAO1*aro*A mutant is auxotrophic for aromatic amino acids and must be cultivated with aromatic amino acid supplement. Under these conditions, the wild-type PAO1 strain entered log phase in 2 h, but the PAO1*aro*A mutant strain grew more slowly, entering log phase in 5 h (Figure S8). Nevertheless, when we compared rhamnolipid production after 48 h of fermentation, there was no significant difference between the wild-type PAO1 and PAO1*aro*A mutant strains (Figure 6B).

To increase rhamnolipid production in the PAO1*aro*A mutant, we introduced a plasmid carrying *rhl*AB, which participates in the biosynthesis of this biosurfactant (Ochsner et al., 1994), and the *est*A gene, which encodes an autotransporter protein located in the outer membrane (Wilhelm et al., 2007) (Figure S9). Overexpression of *rhl*AB and *est*A in wild-type PAO1 and the PAO1*aro*A mutant increased the yield of rhamnolipids (Figure 6B). Using a toluene emulsion assay (Biggins et al., 2014), we tested the emulsive potential of the PAO1*aro*A mutant in the presence of *rhl*AB and *est*A. Visible emulsions formed in the supernatants of both wild-type PAO1 and the PAO1*aro*A mutant (Figure 6C). We also confirmed the stability of the expression plasmid pBBR1-estA-genta-rhlAB, which replicated in the PAO1*aro*A mutant without antibiotic selection (Figure 6D). Thus a safe rhamnolipid producer for industrial fermentation has been established.

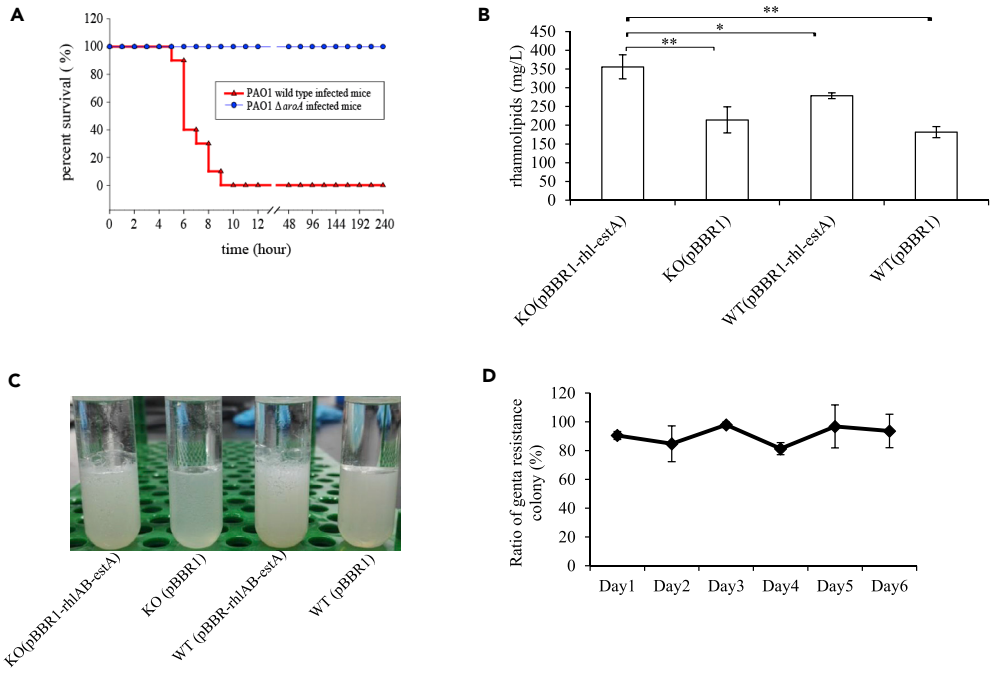

Figure 6. Overexpression of *rhl*AB and *est*A in the PAO1 Mutant for Rhamnolipid Production

(A) The survival rate of BALB/c mice after intraperitoneal injection of wild-type PAO1 and the PAO1*aro*A mutant strain ($1*10^9$ CFU).

(B) Rhamnolipid production in wild-type PAO1 and the PAO1*aro*A mutant from a 2-day fermentation. The statistical analysis used is Student's t test. *$p < 0.05$, **$p < 0.01$.

(C) Emulsification activity of cell culture supernatants. Equal parts of toluene and supernatant were combined in a glass vial, vortexed vigorously, and rested for 2 h.

(D) Plasmid stability in the PAO1aroA mutant. The tested plasmid was pBBRI-estA-genta-rhlAB. This strain was cultured in Murashige and Skoog (MS) medium supplemented with aromatic amino acids without antibiotic, and the number of cells was counted on LB plates with and without gentamycin every day. The ratio of gentamycin-resistant clones to total cells was calculated. Data represent the mean ± SD from three independent experiments.

DISCUSSION

Although the Red system has been applied to engineer the genome of *E. coli* and a number of genetically close species, apparent host-specific factors limit its wider application (Yin et al., 2015). Consequently, we and others have searched for other phage exonuclease/SSAP pairs associated with genetically distant bacterium. This includes the prophage $RecET_{Psy}$ system, which has been used in *P. syringae* so far (Swingle et al., 2010).

Several attempts of recombineering in *P. putida* have been recently reported. However, the enzymes are *lambda* Red (Chen et al., 2016; Cook et al., 2018; Luo et al., 2016) and *rac* RecET (Choi et al., 2018), or an SSAP without an accompanying exonuclease (Aparicio et al., 2016, 2018; Ricaurte et al., 2018). It is well known that the use of SSAPs alone is only effective with single-stranded oligonucleotides and will not mediate the dsDNA homologous recombination events.

Pseudomonas is a large genus including *P. aeruginosa*, *P. chlororaphis*, *P. fluorescens*, *P. pertucinogena*, *P. putida*, *P. stutzeri*, *P. syringae*, and a large number of *Incertae sedis*. In a search for recombineering solutions to cover this broad range, we worked with representatives from four groups, namely, *P. aeruginosa*, *P. fluorescens*, *P. putida*, and *P. syringae*. In addition to $RecET_{Psy}$, we identified another operon in the *Pseudomonas* phage vB_PaeP_Tr60_Ab31 (Latino et al., 2014) (Figure 1). These operons differ from the *E. coli* lambda Red operon (Redγβα) or our previously reported *P. luminescens* operon (Pluγβα) (Yin et al., 2015) because they do not appear to include a Redγ/Pluγ-type inhibitor of the major host exonuclease RecBCD, which protects linear dsDNA ends from degradation and thereby facilitates recombination. Therefore we added Pluγ and Redγ to the TE_{Psy} and BAS systems to evaluate their impact

on recombineering. Owing to apparent toxicity and temperature optima, we did not arrive at a single optimal configuration for all four *Pseudomonas* species. In *P. aeruginosa* PluγTE_{Psy} delivered the best results at 30°C, whereas RedγBAS was the configuration for 37°C. Furthermore, Redγ and Pluγ increased recombineering efficiency in *P. aeruginosa* and *P. fluorescens*, but Redγ was deleterious in *P. putida* and *P. syringae*. We suggest that Redγ likely alters the function of the RecBCD complex in *E. coli*, *P. aeruginosa*, and *P. fluorescens* in the same manner by temporarily blocking its exonuclease activity. However, the interaction between Redγ and RecBCD in *P. syringae* or *P. putida* might proceed differently, potentially to have an effect on RecBCD-mediated genome repair.

Consequently, after evaluating different configurations in four *Pseudomonas* species, we found that the BAS system was functional in all four tested *Pseudomonas* strains and so has the potential to be a generic system for *Pseudomonas* after testing for Pluγ or Redγ functionality.

We report the usefulness of an SSB in a recombineering system. The three-element BAS and four-element hybrid RedγBAS systems are useful genome engineering tools in certain *Pseudomonas* strains. Consequently, we were motivated to explore the utility of S, the phage Ab31 SSB, in both established recombineering paradigms, Red and RecET in LCHR and LLHR applications.

In *E. coli*, S clearly contributed to BA recombination. Addition of S had little impact on Red recombination. However, it substantially enhanced RecET in both LCHR and LLHR assays (Figures 4D and 4E).

SSBs play crucial roles in DNA replication, recombination, DNA damage signaling, and repair in all organisms (Yang et al., 2013). In addition, SSBs can protect ssDNA from further degradation after 5′-3′ exonuclease resection (Meyer and Laine, 1990). SSB also forms a protein interaction platform by recruiting DNA replication and recombination enzymes, such as exonuclease I (Lu et al., 2011) and RecJ (Han et al., 2006). Biochemical studies of different recombination systems have revealed that SSB binds to and removes secondary structures from ssDNA during the presynapsis stage (Kowalczykowski and Krupp, 1987), which facilitates homologous strand pairing. Therefore, an SSB could potentially contribute to recombineering in three ways, namely, protection of ssDNAs involved in recombination from degradation, interaction(s) with the recombination machinery, or removal of secondary structures in ssDNA intermediates. We designed an experiment to test this third possibility to determine if homologous recombination efficiency was affected by secondary structure of the homology arm and whether an SSB could ameliorate the impact. However, on comparison of a homology arm with notable secondary structure to an arm with moderate secondary structure, there was no bias with or without SSB overexpression in the recombineering host (Figures 7A–7C). Although further studies are necessary to elucidate the biological role of SSB in recombineering, we suggest that the variable contributions of a RecBCD inhibitor or an SSB in different contexts reflect different recombination susceptibilities to double- or single-stranded exonucleases.

Based on the RedγBAS and PluγTE_{Psy} recombineering systems, we constructed two *P. aeruginosa* mutants, PABMT and PAO1*aro*A. PABMT could postpone the egg stage for *C. elegans* but was still pathogenic to BALB/c mice, suggesting the presence of additional pathogenic factors. PAO1*aro*A is a highly attenuated strain (Figure 6A) with potential for several applications, such as live vaccines (Priebe et al., 2002). In the present study, the highly attenuated mutant was used to produce rhamnolipid biosurfactants. Rhamnolipids are surface-active secondary metabolites produced by *P. aeruginosa* or related species in the stationary phase (Zhang et al., 2012). In the last decade, these molecules have emerged as a promising class of biosurfactants for several applications, such as moisturizers, lubricants, and shampoos (Dobler et al., 2016). Rhamnolipids are also effective in the bioremediation of organic and heavy-metal-polluted sites. Consequently, various efforts, including heterologous expression of *rhl*AB, have been made to establish high-yield rhamnolipid-producing strains. However, *P. aeruginosa* remains the best rhamnolipid producer. Based on the attenuated strain, further modifications to increase secondary metabolite production would involve the overexpression of proteins that participate in biosynthetic and/or regulatory pathways (Dobler et al., 2016). As expected, the overexpression of *rhl*AB and *est*A in wild-type PAO1 and the PAO1*aro*A mutant strain increased the yield of rhamnolipids (Figure 6B). The rhamnosyltransferase 1 complex (RhlAB) is the key enzyme responsible for transferring the rhamnose moiety to the β-hydroxyalkanoic acid moiety during rhamnolipid biosynthesis (Wang et al., 2007). Rhamnolipid production in *P. aeruginosa* is regulated by the hierarchical quorum-sensing systems (LasI/R and RhlI/R systems) (Soberón-Chávez et al., 2005). EstA

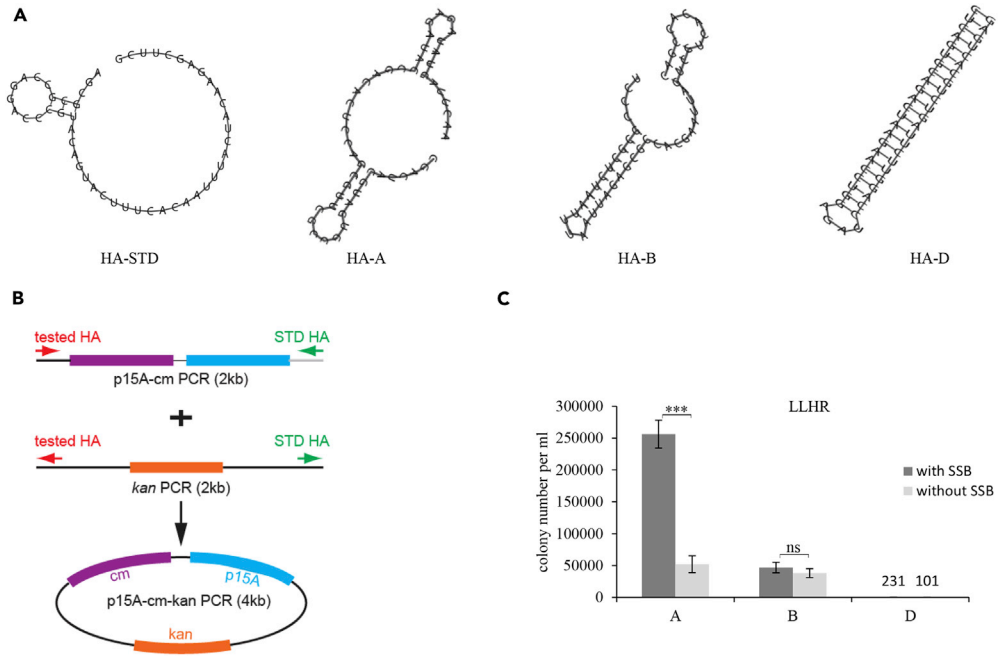

Figure 7. Effects of Secondary Structure on Recombineering with or without SSB

(A) Secondary structure predictions of the standard homology arm (HA-STD) and tested homology arms (HA-A, HA-B, and HA-D) from the RNAfold Webserver (http://rna.tbi.univie.ac.at/cgi-bin/RNAWebSuite/RNAfold.cgi) (Mathews et al., 2004).

(B) Diagram of the LLHR assay in *E. coli* (Fu et al., 2012). Each end of the kan-PCR product has a 50-bp homology arm to the p15A-cm PCR product between the chloramphenicol gene (cm) and the p15A origin (indicated by red and green arrows).

(C) Results from the LLHR assay depicted in (B) upon expression of full-length RecE, RecT, and Redγ with or without SSB. Colonies were selected on kanamycin or chloramphenicol plates and counted.

Data represent the mean ± SD from three independent experiments. The statistical analysis used is Student's t test. *$p < 0.05$, ns: not significant.

indirectly influences the synthesis of quorum-sensing molecules by providing the cells with fatty acids (Riedel et al., 2003).

For *P. aeruginosa* PAO1, after electroporation the recombinants were selected on LB agar plates supplemented with gentamycin (15 μg/mL). There were false-positive colonies, which were smaller. According to colony PCR using the internal primer pairs binding to the gentamycin resistance gene, this was not random integration of the cassette (Figure S10). As negative controls we observed that there were gentamycin-resistant colonies of *P. aeruginosa* after electroporation without adding DNA. Most likely the intrinsic multidrug resistance mechanisms of *P. aeruginosa* were enhanced after electroporation as a stress response. However these false-positive colonies were not problematic for screening, as they did not grow in liquid LB containing gentamycin (15 μg/mL) because of antibiotic selection being more stringent in the liquid medium than in the solid medium (data not shown).

Here, we developed recombineering systems for *Pseudomonas* for several reasons including circumventing the inconvenience of constructing a suicide plasmid with long homology arms for genome engineering, which then requires tedious PCR screening of single-crossover and double-crossover events (Hmelo et al., 2015). Further work to construct efficient recombineering systems for more distantly related gram-negative bacteria may require not only the identification of new Red-like or RecET-like operons but also testing combinations of SSBs and Redγ-like proteins with the phage exonuclease/SSAP pairs.

Limitations of the Study

We evaluated two *Pseudomonas* endogenous phage recombinant systems (BAS and $RecET_{psy}$) in various strains and use the *E. coli* Red and Plu Red recombinant proteins (Redγβα and Pluγβα) as references. These

proteins were expressed using the same inducible promoter and the same plasmid origin. However, we did not assess the expression levels of such proteins, so future experiments are needed to test whether differences in expression levels of these proteins can explain different recombineering efficiencies among strains.

METHODS

All methods can be found in the accompanying Transparent Methods supplemental file.

SUPPLEMENTAL INFORMATION

Supplemental Information can be found online at https://doi.org/10.1016/j.isci.2019.03.007.

ACKNOWLEDGMENTS

The authors thank Vinothkannan Ravichandran for critical reading of the manuscript. This study was supported by grants from the National Natural Science Foundation of China (31570094, 31700004, and 31670097), the Shandong Provincial Natural Science Foundation of China (ZR2018ZC2261, ZR2017ZB0212), the 111 Project (B16030), the Science and Technology Development Program of Suzhou (SYG201507), the Natural Science Foundation of Jiangsu Province (BK20160368), the Key Programs of Frontier Scientific Research of the Chinese Academy of Sciences (QYZDY-SSW-SMC008), the State Key Laboratory of Microbial Technology Open Projects Fund (M2017-05), the Huxiang Youth Excellent (2017RS3029) to J.Y., the Recruitment Program of Global Experts in Shandong University to Y.Z., the Qilu Youth Scholar Startup Funding of SDU to H.W., and the Taishan Scholar Program of Shandong Province to J.F. and H.W.

AUTHOR CONTRIBUTIONS

J.Y., Y.Y., A.F.S., Y.Z., and J.F. designed the study. J.Y. and W.Z. performed the informatic analysis, expression plasmid construction, and recombineering efficiency analysis. Y.G. and R.L. performed the mice and *C. elegans* experiments. C.J., H.W., and A.L. performed rhamnolipid quantification. H.S., X.D., S.L., and H.C. constructed the mutants. J.Y., A.F.S., and J.F. wrote the manuscript.

DECLARATION OF INTERESTS

The authors declare no competing interests.

Received: October 24, 2018
Revised: December 28, 2018
Accepted: March 7, 2019
Published: April 26, 2019

REFERENCES

Aditi, F.Y., Rahman, S.S., and Hossain, M.M. (2017). A study on the microbiological status of mineral drinking water. Open Microbiol. J. *11*, 31–44.

Antoine, R., and Locht, C. (1992). Isolation and molecular characterization of a novel broad-host-range plasmid from Bordetella bronchiseptica with sequence similarities to plasmids from Gram-positive organisms. Mol. Microbiol. *6*, 1785–1799.

Aparicio, T., de Lorenzo, V., and Martínez-García, E. (2018). CRISPR/Cas9-based counterselection boosts recombineering efficiency in *Pseudomonas putida*. Biotechnol. J. *13*, 1700161.

Aparicio, T., Jensen, S.I., Nielsen, A.T., de Lorenzo, V., and Martínez-García, E. (2016). The Ssr protein (T1E_1405) from *Pseudomonas putida* DOT-T1E enables oligonucleotide-based recombineering in platform strain *P. putida* EM42. Biotechnol. J. *11*, 1309–1319.

Beloin, C., Deighan, P., Doyle, M., and Dorman, C.J. (2003). Shigella flexneri 2a strain 2457T expresses three members of the H-NS-like protein family: characterization of the Sfh protein. Mol. Genet. Genom. *270*, 66–77.

Biggins, J.B., Kang, H.-S., Ternei, M.A., DeShazer, D., and Brady, S.F. (2014). The chemical arsenal of Burkholderia Pseudomallei is essential for pathogenicity. J. Am. Chem. Soc. *136*, 9484–9490.

Bunny, K., Liu, J., and Roth, J. (2002). Phenotypes of lexA mutations in Salmonella enterica: evidence for a lethal lexA null phenotype due to the Fels-2 prophage. J. Bacteriol. *184*, 6235–6249.

Carroll, S.F., and Collier, R.J. (1987). Active site of *Pseudomonas aeruginosa* exotoxin A. Glutamic acid 553 is photolabeled by NAD and shows functional homology with glutamic acid 148 of diphtheria toxin. J. Biol. Chem. *262*, 8707–8711.

Chen, Z., Ling, W., and Shang, G. (2016). Recombineering and I-SceI-mediated *Pseudomonas putida* KT2440 scarless gene deletion. FEMS Microbiol. Lett. *363*, fnw231.

Choi, K.R., Cho, J.S., Cho, I.J., Park, D., and Lee, S.Y. (2018). Markerless gene knockout and integration to express heterologous biosynthetic gene clusters in *Pseudomonas putida*. Metab. Eng. *47*, 463–474.

Cook, T.B., Rand, J.M., Nurani, W., Courtney, D.K., Liu, S.A., and Pfleger, B.F. (2018). Genetic tools for reliable gene expression and recombineering in *Pseudomonas putida*. J. Ind. Microbiol. *45*, 517–527.

Court, R., Cook, N., Saikrishnan, K., and Wigley, D. (2007). The crystal structure of lambda-Gam protein suggests a model for RecBCD inhibition. J. Mol. Biol. *371*, 25–33.

Derbise, A., Lesic, B., Dacheux, D., Ghigo, J.M., and Carniel, E. (2003). A rapid and simple method for inactivating chromosomal genes in Yersinia. FEMS Microbiol. Lett. *38*, 113–116.

Dobler, L., Vilela, L.F., Almeida, R.V., and Neves, B.C. (2016). Rhamnolipids in perspective: gene regulatory pathways, metabolic engineering, production and technological forecasting. New Biotechnol. *33*, 123–135.

Dong, H., Tao, W., Gong, F., Li, Y., and Zhang, Y. (2013). A functional recT gene for recombineering of *Clostridium*. J. Biotechnol. *173*, 65–67.

Egan, M., Ramirez, J., Xander, C., Upreti, C., and Bhatt, S. (2016). Lambda red-mediated recombineering in the attaching and effacing pathogen Escherichia albertii. Biol. Proced. Online *18*, 3.

Egan, S.M., and Schleif, R.F. (1993). A regulatory cascade in the induction of rhaBAD. J. Mol. Biol. *234*, 87–98.

Egan, S.M., and Schleif, R.F. (1994). DNA-dependent renaturation of an insoluble DNA binding protein. J. Mol. Biol. *243*, 821–829.

Erler, A., Wegmann, S., Elie-Caille, C., Bradshaw, C.R., Maresca, M., Seidel, R., Habermann, B., Muller, D.J., and Stewart, A.F. (2009). Conformational adaptability of Redβ during DNA annealing and implications for its structural relationship with Rad52. J. Mol. Biol. *391*, 586–598.

EUZéBY, J.P. (1997). List of bacterial names with standing in nomenclature: a folder available on the internet. Int. J. Syst. Evol. Microbiol. *47*, 590–592.

Fu, J., Bian, X., Hu, S., Wang, H., Huang, F., Seibert, P.M., Plaza, A., Xia, L., Müller, R., Stewart, A.F., et al. (2012). Full-length RecE enhances linear-linear homologous recombination and facilitates direct cloning for bioprospecting. Nat. Biotechnol. *30*, 440–446.

Fu, J., Teucher, M., Anastassiadis, K., Skarnes, W., and Stewart, A.F. (2010). Chapter eight - a recombineering pipeline to make conditional targeting constructs. In Methods in Enzymology, M.W. Paul and M.S. Philippe, eds. (Academic Press), pp. 125–144.

Gomes, N.C.M., Kosheleva, I.A., Abraham, W.-R., and Smalla, K. (2005). Effects of the inoculant strain *Pseudomonas putida* KT2442 (pNF142) and of naphthalene contamination on the soil bacterial community. FEMS Microbiol. Ecol. *54*, 21–33.

Han, E.S., Cooper, D.L., Persky, N.S., Sutera, V.A., Whitaker, R.D., Montello, M.L., and Lovett, S.T. (2006). RecJ exonuclease: substrates, products and interaction with SSB. Nucleic Acids Res. *34*, 1084–1091.

Hmelo, L.R., Borlee, B.R., Almblad, H., Love, M.E., Randall, T.E., Tseng, B.S., Lin, C., Irie, Y., Storek, K.M., Yang, J.J., et al. (2015). Precision-engineering the *Pseudomonas aeruginosa* genome with two-step allelic exchange. Nat. Protoc. *10*, 1820–1841.

Jinno, Y., Chaudhary, V.K., Kondo, T., Adhya, S., FitzGerald, D.J., and Pastan, I. (1988). Mutational analysis of domain I of Pseudomonas exotoxin. Mutations in domain I of Pseudomonas exotoxin which reduce cell binding and animal toxicity. J. Biol. Chem. *263*, 13203–13207.

Kowalczykowski, S.C., and Krupp, R.A. (1987). Effects of Escherichia coli SSB protein on the single-stranded DNA-dependent ATPase activity of Escherichia coli RecA protein. J. Mol. Biol. *193*, 97–113.

Latino, L., Essoh, C., Blouin, Y., Vu Thien, H., and Pourcel, C. (2014). A novel *Pseudomonas aeruginosa* bacteriophage, Ab31, a Chimera formed from temperate Phage PAJU2 and *P. putida* Lytic Phage AF: characteristics and mechanism of bacterial resistance. PLoS One *9*, e93777.

Lau, G.W., Hassett, D.J., Ran, H., and Kong, F. (2004). The role of pyocyanin in *Pseudomonas aeruginosa* infection. Trends Mol. Med. *10*, 599–606.

Lu, D., Myers, A.R., George, N.P., and Keck, J.L. (2011). Mechanism of exonuclease I stimulation by the single-stranded DNA-binding protein. Nucleic Acids Res. *39*, 6536–6545.

Luo, X., Yang, Y., Ling, W., Zhuang, H., Li, Q., and Shang, G. (2016). *Pseudomonas putida* KT2440 markerless gene deletion using a combination of λ Red recombineering and Cre/loxP site-specific recombination. FEMS Microbiol. Lett. *363*, fnw014.

Mahajan-Miklos, S., Tan, M.-W., Rahme, L.G., and Ausubel, F.M. (1999). Molecular mechanisms of bacterial virulence elucidated using a *Pseudomonas aeruginosa* Caenorhabditis elegans pathogenesis model. Cell *96*, 47–56.

Maresca, M., Erler, A., Fu, J., Friedrich, A., Zhang, Y., and Stewart, A.F. (2010). Single-stranded heteroduplex intermediates in lambda Red homologous recombination. BMC Mol. Biol. *29*, 11–54.

Mathews, D.H., Disney, M.D., Childs, J.L., Schroeder, S.J., Zuker, M., and Turner, D.H. (2004). Incorporating chemical modification constraints into a dynamic programming algorithm for prediction of RNA secondary structure. Proc. Natl. Acad. Sci. U S A *101*, 7287–7292.

McEwan, D.L., Kirienko, N.V., and Ausubel, F.M. (2012). Host translational inhibition by *Pseudomonas aeruginosa* exotoxin a triggers an immune response in Caenorhabditis elegans. Cell Host Microbe *11*, 364–374.

McIver, K., Kessler, E., and Ohman, D.E. (1991). Substitution of active-site His-223 in *Pseudomonas aeruginosa* elastase and expression of the mutated lasB alleles in Escherichia coli show evidence for autoproteolytic processing of proelastase. J. Bacteriol. *173*, 7781–7789.

Meyer, R.R., and Laine, P.S. (1990). The single-stranded DNA-binding protein of Escherichia coli. Microbiol. Rev. *54*, 342–380.

Murphy, K. (1998). Use of bacteriophage lambda recombination functions to promote gene replacement in Escherichia coli. J. Bacteriol. *180*, 2063–2071.

Murphy, K.C. (1991). Lambda Gam protein inhibits the helicase and chi-stimulated recombination activities of Escherichia coli RecBCD enzyme. J. Bacteriol. *173*, 5808–5821.

Muyrers, J.P.P., Zhang, Y., Buchholz, F., and Stewart, A.F. (2000). RecE/RecT and Redalpha/Redbeta initiate double-stranded break repair by specifically interacting with their respective partners. Genes Dev. *14*, 1971–1982.

Muyrers, J.P.P., Zhang, Y., Testa, G., and Stewart, A.F. (1999). Rapid modification of bacterial artificial chromosomes by ET-recombination. Nucleic Acids Res. *27*, 1555–1557.

Ochsner, U.A., Fiechter, A., and Reiser, J. (1994). Isolation, characterization, and expression in Escherichia coli of the *Pseudomonas aeruginosa* rhlAB genes encoding a rhamnosyltransferase involved in rhamnolipid biosurfactant synthesis. J. Biol. Chem. *269*, 19787–19795.

Paulsen, I.T., Press, C.M., Ravel, J., Kobayashi, D.Y., Myers, G.S.A., Mavrodi, D.V., DeBoy, R.T., Seshadri, R., Ren, Q., Madupu, R., et al. (2005). Complete genome sequence of the plant commensal *Pseudomonas fluorescens* Pf-5. Nat. Biotechnol. *23*, 873–878.

Pijkeren, J.P., and Britton, R.A. (2012). High efficiency recombineering in lactic acid bacteria. Nucleic Acids Res. *40*, e76.

Pijkeren, J.P., Neoh, K.M., Sirias, D., Findley, A.S., and Britton, R.A. (2012). Exploring optimization parameters to increase ssDNA recombineering in *Lactococcus lactis* and *Lactobacillus reuteri*. Bioengineered *3*, 209–217.

Priebe, G.P., Brinig, M.M., Hatano, K., Grout, M., Coleman, F.T., Pier, G.B., and Goldberg, J.B. (2002). Construction and characterization of a live, attenuated aroA deletion mutant of *Pseudomonas aeruginosa* as a candidate intranasal vaccine. Infect. Immun. *70*, 1507–1517.

Ricaurte, D.E., Martínez-García, E., Nyerges, Á., Pál, C., Lorenzo, V., and Aparicio, T. (2018). A standardized workflow for surveying recombinases expands bacterial genome-editing capabilities. Microb. Biotechnol. *11*, 176–188.

Riedel, K., Talker-Huiber, D., Givskov, M., Schwab, H., and Eberl, L. (2003). Identification and characterization of a GDSL esterase gene located proximal to the swr quorum-sensing system of Serratia liquefaciens MG1. Appl. Environ. Microbiol. *69*, 3901–3910.

Rossi, M.-S., Paquelin, A., Ghigo, J.M., and Wandersman, C. (2003). Haemophore-mediated signal transduction across the bacterial cell envelope in Serratia marcescens: the inducer and the transported substrate are different molecules. Mol. Microbiol. *48*, 1467–1480.

Savoia, D. (2014). New perspectives in the management of *Pseudomonas aeruginosa* infections. Future Microbiol. *9*, 917–928.

Sharan, S.K., Thomason, L.C., Kuznetsov, S.G., and Court, D.L. (2009). Recombineering: a homologous recombination-based method of genetic engineering. Nat. Protoc. *4*, 206–223.

Siegall, C.B., Chaudhary, V.K., FitzGerald, D.J., and Pastan, I. (1989). Functional analysis of domains II, Ib, and III of Pseudomonas exotoxin. J. Biol. Chem. *264*, 14256–14261.

Soberón-Chávez, G., Lépine, F., and Déziel, E. (2005). Production of rhamnolipids by

Pseudomonas aeruginosa. Appl. Environ. Microbiol. *68*, 718–725.

Stover, C.K., Pham, X.Q., Erwin, A.L., Mizoguchi, S.D., Warrener, P., Hickey, M.J., Brinkman, F.S.L., Hufnagle, W.O., Kowalik, D.J., Lagrou, M., et al. (2000). Complete genome sequence of *Pseudomonas aeruginosa* PAO1, an opportunistic pathogen. Nature *406*, 959–964.

Sun, Z., Deng, A., Hu, T., Wu, J., Sun, Q., Bai, H., Zhang, G., and Wen, T. (2015). A high-efficiency recombineering system with PCR-based ssDNA in Bacillus subtilis mediated by the native phage recombinase GP35. Appl. Environ. Microbiol. *99*, 5151–5162.

Swingle, B., Bao, Z., Markel, E., Chambers, A., and Cartinhour, S. (2010). Recombineering using RecTE from *Pseudomonas syringae*. Appl. Environ. Microbiol. *76*, 4960–4968.

Szczepańska, A.K. (2009). Bacteriophage-encoded functions engaged in initiation of homologous recombination events. Crit. Rev. Microbiol. *35*, 197–220.

Validov, S., Kamilova, F., Qi, S., Wang, J.J., Makarova, N., and Lugtenberg, B. (2007). Selection of bacteria able to control Fusarium oxysporum f. sp. radicis-lycopersici in stonewool substrate. J. Appl. Microbiol. *102*, 461–471.

Van Kessel, J.C., and Hatfull, G.F. (2006). Recombineering in *Mycobacterium tuberculosis*. Nat. Methods *4*, 147–152.

Wang, J., Sarov, M., Rientjes, J., Fu, J., Hollak, H., Kranz, H., Xie, W., Stewart, A.F., and Zhang, Y. (2006). An improved recombineering approach by adding RecA to lambda Red recombination. Mol. Biotechnol. *32*, 43–53.

Wang, Q., Fang, X., Bai, B., Liang, X., Shuler, P.J., Goddard, W.A., and Tang, Y. (2007). Engineering bacteria for production of rhamnolipid as an agent for enhanced oil recovery. Biotechnol. Bioeng. *98*, 842–853.

Wilhelm, S., Gdynia, A., Tielen, P., Rosenau, F., and Jaeger, K.-E. (2007). The autotransporter esterase EstA of *Pseudomonas aeruginosa* is required for rhamnolipid production, cell motility, and biofilm formation. J. Bacteriol. *189*, 6695–6703.

Xin, X.-F., and He, S.Y. (2013). *Pseudomonas syringae* pv. tomato DC3000: a model pathogen for probing disease susceptibility and hormone signaling in plants. Annu. Rev. Phytopathol. *51*, 473–498.

Yang, P., Wang, J., and Qi, Q. (2015). Prophage recombinases-mediated genome engineering in *Lactobacillus plantarum*. Microb. Cell Fact. *14*, 1–11.

Yang, S.H., Zhou, R., Campbell, J., Chen, J., Ha, T., and Paull, T.T. (2013). The SOSS1 single-stranded DNA binding complex promotes DNA end resection in concert with Exo1. EMBO J. *32*, 126–139.

Yang, Z.-S., Ma, L.-Q., Zhu, K., Yan, J.-Y., Bian, L., Zhang, K.-Q., and Zou, C.-G. (2016). Pseudomonas toxin pyocyanin triggers autophagy: implications for pathoadaptive mutations. Autophagy *12*, 1015–1028.

Yin, J., Zhu, H., Xia, L., Ding, X., Hoffmann, T., Hoffmann, M., Bian, X., Müller, R., Fu, J., Stewart, A.F., et al. (2015). A new recombineering system for Photorhabdus and *Xenorhabdus*. Nucleic Acids Res. *43*, e36.

Zhang, L., Veres-Schalnat, T.A., Somogyi, A., Pemberton, J.E., and Maier, R.M. (2012). Fatty acid cosubstrates provide β-Oxidation precursors for rhamnolipid biosynthesis in *Pseudomonas aeruginosa*, as evidenced by isotope tracing and gene expression assays. Appl. Environ. Microbiol. *78*, 8611–8622.

Zhang, Q., Xiao, Q., Xu, J., Tong, Y., Wen, J., Chen, X., and Wei, L. (2015). Effect of retS gene on antibiotics production in *Pseudomonas fluorescens* FD6. Microbiol. Res. *180*, 23–29.

Zhang, Y., Buchholz, F., Muyrers, J.P.P., and Stewart, A.F. (1998). A new logic for DNA engineering using recombination in Escherichia coli. Nat. Genet. *20*, 123–128.

Zhang, Y., Muyrers, J.P.P., Testa, G., and Stewart, A.F. (2000). DNA cloning by homologous recombination in Escherichia coli. Nat. Biotechnol. *18*, 1314–1317.

Zhao, F., Cui, Q., Han, S., Dong, H., Zhang, J., Ma, F., and Zhang, Y. (2015). Enhanced rhamnolipid production of *Pseudomonas aeruginosa* SG by increasing copy number of rhlAB genes with modified promoter. RSC Adv. *5*, 70546–70552.

ISCI, Volume *14*

Supplemental Information

Single-Stranded DNA-Binding Protein and Exogenous RecBCD Inhibitors Enhance Phage-Derived Homologous Recombination in *Pseudomonas*

Jia Yin, Wentao Zheng, Yunsheng Gao, Chanjuan Jiang, Hongbo Shi, Xiaotong Diao, Shanshan Li, Hanna Chen, Hailong Wang, Ruijuan Li, Aiying Li, Liqiu Xia, Yulong Yin, A. Francis Stewart, Youming Zhang, and Jun Fu

Supplementary information

TRANSPARENT METHOD

Strains, plasmids and reagents

The bacterial strains and plasmids used are listed in **Table S1 and Table S2**. The expression plasmids used to evaluate homologous recombination efficiencies are based on the pBBR1 origin(Antoine and Locht, 1992) and the *rha*R-*rha*S P_{Rha} promoter(Egan and Schleif, 1993, 1994). The plasmids were constructed by recombineering either in GB08-red or in GB05-dir(Fu et al., 2012; Fu et al., 2010). Oligonucleotides were synthesized by Sangon Biotech (Shanghai) Co., Ltd., in China (**Table S3**). Phusion polymerase, restriction enzymes and DNA markers were purchased from New England Biolabs (Massachusetts, USA). Antibiotics were supplied by Invitrogen (Massachusetts, USA). *E. coli, P. aeruginosa, P. fluorescens and P. putida* were cultured in Luria-Bertani (LB) broth or on LB agar plates (1.2% agar)(Bertani, 1951); *P. syringae* was cultured in Kings B medium(King et al., 1954). The concentrations of the required antibiotics are listed in **Table S4.**

Preparation of expression plasmid

The expression plasmids used to evaluate homologous recombination efficiencies are based on the pBBR1 origin(Antoine and Locht, 1992) and the *rha*R-*rha*S P_{Rha} promoter(Egan and Schleif, 1993, 1994), and constructed by four steps. First, pGDFG10 (unpublished in our lab), named pBBR1-Rha-TE_{Psy}-kan in the present study, was digested by XmnI, and the restriction fragment was purified by agarose gel. Second, *redγβα* and *pluγβα* were PCR amplified from pSC101-BAD-*redγβαA*-tet(Fu et al., 2010) and pSC101-BAD-*pluγβα*-amp(Yin et al., 2015), respectively. The function genes of BAS were synthesised from GENEWIZ (Suzhou) Co., Ltd., in China. Third, the restriction fragment and function genes were co-transformation in GB05-dir(Fu et al., 2012) by recombineering to construct pBBR1-Rha-redγβα-Kan, pBBR1-Rha-pluγβα-kan and pBBR1-Rha-BAS-kan. Fourth, the *redγ* and *pluγ* was inserted into pBBR1-Rha-TE_{Psy}-kan and pBBR1-Rha-BAS-kan by recombineering in GB08-red(Fu et al., 2010).

Electrocompetent cell preparation and recombineering

Various expression plasmids were electroporated into *E. coli* GB2005, *P. aeruginosa* PAO1, *P. fluorescens* pf5, *P. syringae* DC3000, and *P. putida* KT2440. *E. coli* electrocompetent cells were prepared as reported previously(Fu et al., 2010). For *P. aeruginosa, P. fluorescens, P. syringae* and *P. putida*, overnight cultures containing the expression plasmids were diluted into 1.3 mL of LB medium with the appropriate antibiotics. The starting OD_{600} values were approximately 0.085. Fresh cultures were grown at 30°C or 37°C according to the optimum growth temperature for each strain and at 950 rpm for an appropriate amount of time until the log phase began for each strain. After the addition of the inducer L-rhamnose to a final concentration of 2.5 mg mL^{-1}, the cells were grown at 30°C or 37°C and 950 rpm for 40 min. Cells were then centrifuged for 30 s at 9500 rpm at room temperature. The supernatants were discarded, and the cell pellets were resuspended in 1 mL of ddH_2O and centrifuged. The washing procedure was repeated one more time. Then, cells were resuspended in 30 µL of ddH_2O, and DNA was added. For the experiments shown in **Figure 3B-H** and **Figure 4B and C**, 1.5 µg of PCR product was used. Two to five micrograms of PCR product were used for the genome engineering of *P. aeruginosa, P. fluorescens* and *P. syringae*. Electroporation was performed using 1-mm cuvettes and an Eppendorf 2510 electroporator set at 1250 V. One millilitre of the appropriate medium was added after electroporation. The cells were incubated at 30°C for 100 min or 37°C for 60 min with shaking and then spread on plates containing the appropriate antibiotics.

***P. aeruginosa* virulence assays in BALB/c mice and *Caenorhabditis elegans* (*C. elegans*)**

Wild-type *P. aeruginosa* PAO1 and the PAO1*aro*A mutant ($1*10^9$ CFU) were injected intraperitoneally into the mice. Mice were observed for mortality for a period of 7 days. For the *C. elegans* assay, the wild-type PAO1 strain and PABMT mutants ($1*10^8$ CFU) were spread on Nematode Growth Medium (NGM) (3 g L^{-1} NaCl, 17 g L^{-1} agar, 2.5 g

L^{-1} peptone, 5 mg L^{-1} cholesterol, 1 mM $MgSO_4$, 1 mM $CaCl_2$, 2.7 g L^{-1} KH_2PO_4, 0.9 g L^{-1} K_2HPO_4, pH 6.0) plates. Plates were incubated at 37°C for 18-24 h and then placed at room temperature for 8-12 h. Fifteen to twenty L4 stage *C. elegans* were placed on the assay plate, which was then incubated at 16°C. Each independent assay consisted of three replicates. Worm phenotypes were observed by microscopy after 5 days.

Rhamnolipid quantification

Wild-type *P. aeruginosa* PAO1 and mutant strains were first grown in LB broth with 10 μg mL^{-1} gentamycin for 24 h at 37°C with shaking, then diluted 1:10 into mineral salt medium(Wang et al., 2007) supplemented with aromatic amino acids without antibiotics and finally incubated for 2 days.

Rhamnolipid quantification was based on a previously described method(Wang et al., 2007) with slight modifications. Cells were centrifuged for 60 s at 13200 rpm after fermentation, and 1 mL of the supernatant was then extracted with 1 mL of ethyl ether. The organic phase was evaporated to dryness, and 0.1 mL of ddH_2O was added. The sample was diluted 1:10 in a solution containing 0.19% orcinol in 53% H_2SO_4. After heating for 30 min at 80°C, the samples were cooled at room temperature, and the OD_{421} was measured(Koch et al., 1991). The rhamnolipid concentration was calculated using a standard curve for L-rhamnose (0-50 mg L^{-1}) and expressed in triplicate as the rhamnose concentration.

Animals

Male BALB/c mice were provided by the School of Medicine of Shandong University. All male mice were housed under specific pathogen-free conditions within the animal facility. Mice were 6-8 weeks old at the start of the experiments.

Statistical analyses

All data were analysed by two-tailed Student's t-test and were conducted in Prism. A P-value that is less than 0.05 is considered statistically significant.

Ethics statement

All mice experiments in this study were approved and supervised by the Institutional Animal Care and Use Committee of Animal Laboratory Center of Shandong University.

Table S1. Bacterial strains: *Escherichia coli*, *Pseudomonas aeruginosa*, *Pseudomonas fluorescens*, *Pseudomonas syringae*, *Pseudomonas putida*, related to Figure 2, 3, 4 and 5.

Strain	**Genome type**	**Optimum growth temperature (ºC)**	**References or sources**
GB2005	F-*mcr*A Δ(*mrr-hsd*RMS-*mcr*BC) φ80*lac*ZΔM15 Δ*lac*X74 *rec*A1 *end*A1 *ara*D139 Δ(ara, leu)7697 *gal*U *gal*K λ *rps*L *nup*G *fhu*A::IS2 *rec*ET *redα*, phage T1-resistant (*E. coli*)	37	(Fu, 2010)
GB05-dir	GB2005, araC-BAD-ETγA (*E. coli*)	37	(Fu et al., 2012)
GB08-red	GB2005, araC-BAD-γβαA, ΔlacZ (*E. coli*)	37	(Fu, 2010)
P. aeruginosa PAO1	Wild-type strain of *Pseudomonas aeruginosa*	37	(Stover et al., 2000)
PAO1*aro*A	*Pseudomonas aeruginosa* PAO1, Δ*aro*A	37	This study
PABMT	*Pseudomonas aeruginosa* PAO1, Δ*phn*AB, Δ*las*B, Δ*mdo*H and *tox*A_{E578D}	37	This study
P. fluorescens pf5	Wild-type strain of *Pseudomonas fluorescens pf5*	30	(Paulsen et al., 2005)
PF5*ret*S	*Pseudomonas fluorescens pf5*, Δ*ret*S	30	This study
P. syringae DC3000	Wild-type strain of *Pseudomonas syringae pv. tomato str.* DC3000	30	(Buell et al., 2003)
P. syringae BGC6	P_{genta} insertion for expression of gene cluster BGC6 in *Pseudomonas syringae pv. tomato str.* DC3000, GentaR	30	This study
P. putida KT2440	Wild-type strain of *Pseudomonas putida* KT2440	30	(Gross et al., 2006)

Table S2. Expression plasmids and PCR template, related to Figure 3 and 4.

Plasmid	**Characteristics**	**References or sources**
pBBR1-Rha-redγβα-Kan	*redγβα* under Rha promoter	This study
pBBR1-Rha-pluγβα-kan	*pluγβα* under Rha promoter	This study
pBBR1-Rha-TE_{Psy}-kan	*rec*TE_{Psy} under Rha promoter	This study
pBBR1-Rha-pluγTE_{Psy}-kan	*rec*TE_{Psy} and *pluγ* under Rha promoter	This study
pBBR1-Rha-redγTE_{Psy}-kan	*rec*TE_{Psy} and *redγ* under Rha promoter	This study
pBBR1-Rha-BAS-kan	BAS gene under Rha promoter	This study
pBBR1-Rha-pluγBAS-kan	BAS gene and *pluγ* under Rha promoter	This study
pBBR1-Rha-redγBAS-kan	BAS gene and *redγ* under Rha promoter	This study
pRK2-apra-cm	PCR templates to amplify apraR gene	This study
pEX18Gm	PCR templates to amplify sacB-gentaR gene	(Ni et al., 2008)
pR6K-Tps-gentaR-tetR-T7RP	PCR templates to amplify lox71-gentaR-lox66 or gentaR gene	(Bian et al., 2012)
pSC101-BAD-ETg-tet	*recET* and *redγ* under BAD promoter	(Fu et al., 2012)
pSC101-BAD-ETgSSB_{E_coli} -tet	*recET*, *redγ* and SSB from *E. coli* genome under BAD promoter	This study
pSC101-BAD-ETg$SSB_{F_plasmid}$-tet	*recET*, *redγ* and SSB from *E. coli* F plasmid under BAD promoter	This study

Table S3. Oligonucleotides, related to Figure 5.

Gene	Primers	5’ - 3’	Application
pluγTE	*pluγ-TE*-3	ACATGCAAATTTTGATCGTGCGATACGGACGCAACGTTTCTTGCGGACATATGATGGCCTCCTTCATATATCCTCCATTTTTAC	Expression plasmid
	pluγ-TE-35	GCGCTTTTTAGACTGGTCGTAATGAACAATTCTTAAGAAGGAGATATACATATGAACCCATATGCAGTTTATG	
redγTE	*redγ-TE*-3	ACATGCAAATTTTGATCGTGCGATACGGACGCAACGTTTCTTGCGGACATATGATGGCCTCCTTTATACCTCTGAATCAATATC	Expression plasmid
	redγ-TE-5	GCGCTTTTTAGACTGGTCGTAATGAACAATTCTTAAGAAGGAGATATACATATGGATATTAATACTGAAACT	
pluγBAS	*pluγ-BAS-3*	TCGTAGCGCGTGGCGAACTTCGTCAGGAGCGGTGTTAGTGCAGTTCCCATCACTAGTCCTCCTTCATATATCCTCCATTTTTAC	Expression plasmid
	pluγ-BAS-5	GCGCTTTTTAGACTGGTCGTAATGAACAATTCTTAAGAAGGAGATATACATATGAACCCATATGCAGTTTATG	
redγBAS	*redγ-BAS-3*	TCGTAGCGCGTGGCGAACTTCGTCAGGAGCGGTGTTAGTGCAGTTCCCATCACTAGTCCTCCTTTATACCTCTGAATCAATATC	Expression plasmid
	redγ-BAS-5	GCGCTTTTTAGACTGGTCGTAATGAACAATTCTTAAGAAGGAGATATACATATGGATATTAATACTGAAACT	
*aro*A-genta-loxM	*aro*A-genta-loxM-3	CACCCGCGGCGTAGAGCCCGGCGAGCAACAGGCAGGACTTCACCTGGGCGCTGGCCATCGGCATGTCGTAATGCAAGCTGAATTACATTCCCAACCG	*Aro*A Knock-out
	*aro*A-genta-loxM-5	CAAGTCGATTTCCCATCGCTCGATCATGCTCGGCTCCCTGGCCGAAGGCACCACCGAAGTGGAGGGCTTCCTCGACAACTTAAATGTGAAAGTGGGTC	
AB-genta-loxM	*AB*-genta-LoxM-3	TTCTCCAGCAGACGCTGGCCGTGGGTGGTGAGAATCGACTCGGGATGGAACTGCAAGCCCAGCTGTCGATTGCGCCAACTTAAATGTGAAAGTGGGTC	*phnAB* Knock-out
	AB-genta-LoxM-5	CAATTGGGGGAAAAGGGGGGTTACCGATGATGAACATGCCGTTGCGCGCTAGCGTCGCGCAGGCCAGTCGCCCATAGCTGAATTACATTCCCAACCG	
lasB-genta-loxM	*lasB*-genta-loxM-3	GAAGGCCTTGCGGGTATCCCAGCCCGGCGAATTGGCCAACAGGTAGAACGCACGGTTGTACACGCCGCTGGAGTGTTAGGTGGCGGTACTTGGGTC	*lasB* Knock-out
	lasB-genta-loxM-5	CGCTACATGGACCAGCCCAGCCGCGACGGGCGATCCATCGACAACGCGTCGCAGTACTACAACGGCATCGACGTGATAGACCAGTTGCAATCCAAACG	

mdoH-genta-loxM	*mdoH*-genta-loxM-3	CCTCTTCCCAGACCCGCGTATGCAGGCGCGAAAGTGCTACCGGGTCACTCAACAGAGCCACAACTTAAATGTGAAAGTGGGTC
	mdoH-genta-loxM-5	GACGAGGCGCAGAAGCCACTGAGCGAAACCTGGAGCTATCAGCTGCCTGCCGATGAATAAAGCTGAATTACATTCCCAACCG
retS-genta-loxM	*retS*-genta-loxM-3	TGGAGCATGGTGGGAGCTCACGACTAAAGGAGGGCGAGCGAGAGTTTAACAGGCGCCGCAGAGCCTGTCGGCTCACAACTTAAATGTGAAAGTGGGTC
	retS-genta-loxM-5	GCACACGCCCTTGCCGTGCGGTCATTACGCCGCGCATAGTTATAATCAGGCATCAACCAACGAAGGGATTTCGCCAGCTGAATTACATTCCCAACCG
*tox*A-sacB-genta	*tox*A-sacB-genta-3	GCCGACGTTGCGCGGGTCGGTGGGGATCGCCGAGGGAATCACCACGGTGCGCTCGGCCAGCGGCCAGCCGAGAATTTAGGTGGCGGTACTTGGGTC
	*tox*A-sacB-genta-5	ACGGCTGATCGGCCATCCGCTGCCGCTGCGCCTGGACGCCATCACCGGCCCCGAGGAGGAAGGCGGGCGCCTGGAATAGACCAGTTGCAATCCAAACG
BGC6-apra	*DC3000-BGC6-3*	TCGCTACAACAAGCTGGCCAAAACCTACGCAGCCATGGTCACGCTGGTCTGCAGCCTACGTTGTAGCGGCGATACGAAGGCACGAACCCAGTTGAC
	DC3000-BGC6-5	TACAGAGGACAGTTCATACGAGAAATTTGAGTTTTTCGATGCTTTTTGATTTGATGGCTTCATGCGTAAACATCCTCGAATTGTTAGGTGGCGGTAC
	Pchk-a1	GTTCCAGACTATCGGCTGTA
	Pchk-a2	TGGCGATTCAGGTTCATCAT
	Hchk-a1	GAGAACAGCCTGCGTTACAAC
	Hchk-a2	ATAGTACCTCAGCTGGCGAAC
	Gent-b1	ATGTTACGCAGCAGCAACGA
	Gent-b2	TTAGGTGGCGGTACTTGGGT

mdoH Knock-out
retS Knock-out
*tox*A point mutation
Insertion promoter
Verify the plasmid recombineering (Figure 3)
Verify the genome engineering of mdoH
PCR product in the GentaR sequence

The homology arms are underlined.

Table S4. Antibiotic concentrations used in different strains, related to Figure 3.

Antibiotic (μg/ml) / Strain	Kanamycin [*km*]	Gentamycin [*genta*]	Apramycin [*apra*]	Tetracycline [*tet*]	Ampicillin [*amp*]	Chloramphenicol [*cm*]
E. coli	15	5	30	5	100	15
P. aeruginosa PAO1	300	15	60	50	ND[b]	90
P. fluorescens pf5	10	15	20	35	ND	ND
P. putida KT2440	15	10	40	--[a]	300	ND
P. syringae pv. tomato str. DC3000	15	3	20	3	200	ND

[a]Did not test this antibiotic

[b]Can not use this antibiotic

Table S5. RecBCD sequence alignment between *Pseudomonas* and *E. coli/P. luminescens*, related to Figure 1.

		E. coli			*P. luminescens*		
		Identities	Positives	Gaps	Identities	Positives	Gaps
P. aeruginosa	RecB	499/1254 (40%)	680/1254 (54%)	109/1254 (8%)	506/1259 (40%)	678/1259 (53%)	92/1259 (7%)
	RecC	448/1160 (39%)	619/1160 (53%)	125/1160 (10%)	422/1181 (36%)	604/1181 (51%)	129/1181 (10%)
	RecD	287/670 (43%)	364/670 (54%)	74/670 (11%)	287/670 (43%)	364/670 (54%)	74/670 (11%)
P. fluorescens	RecB	513/1248 (41%)	691/1248 (55%)	127/1248 (10%)	489/1248 (39%)	675/1248 (54%)	96/1248 (7%)
	RecC	443/1112 (40%)	605/1112 (54%)	118/1112 (10%)	433/1168 (37%)	608/1168 (52%)	134/1168 (11%)
	RecD	281/659 (43%)	367/659 (55%)	75/659 (11%)	281/659 (43%)	367/659 (55%)	75/659 (11%)
P. putida	RecB	493/1217 (41%)	675/1217 (55%)	69/1217 (5%)	488/1235 (40%)	677/1235 (54%)	86/1235 (6%)
	RecC	451/1105 (41%)	613/1105 (55%)	94/1105 (8%)	424/1113 (38%)	587/1113 (52%)	99/1113 (8%)
	RecD	291/660 (44%)	384/660 (58%)	70/660 (10%)	291/660 (44%)	384/660 (58%)	70/660 (10%)
P. syringae	RecB	512/1242 (41%)	693/1242 (55%)	105/1242 (8%)	486/1236 (39%)	673/1236 (54%)	80/1236 (6%)
	RecC	444/1145 (39%)	619/1145 (54%)	125/1145 (10%)	426/1164 (37%)	602/1164 (51%)	137/1164 (11%)
	RecD	277/662 (42%)	371/662 (56%)	78/662 (11%)	344/609 (56%)	427/609 (70%)	10/609 (1%)

Results from NCBI blastp (protein-protein BLAST) using default parameters.

Table S6. Induction and preparation of electrocompetent cells for four *Pseudomonas* strains, related to Figure 2 and 3.

		*P. aeruginosa**	*P. putida**	*P. syringae**	*P. fluorescens**
Induction	Time	2h	2h	3h	1h
	OD_{600}	0.30	0.80	0.70	0.15
Electrocompetent cells preparation	Time	2.5h	2.5h	4h	1.5h
	OD_{600}	0.60	1.50	1.10	0.35

* The overnight culture was diluted to OD600 ≈ 0.085 as the starting culture.

Table S7. Pathogenicity of *P. aeruginosa* in mice, related to Figure 5.

	LD50 (*10^8 CFU)[a]	95% confidence intervals (*10^8 CFU)[a]
Wild type	4.141	3.432-4.850
PABMT[b]	4.339	3.552-5.126

[a]. Mortalities were recorded after 12 h, and 50% lethal dose (LD50) values with 95% confidence intervals were determined using SPSS analysis. These results were determined from three independent assays, and five concentrations for each concentration-response experiment were used.

[b]. PABMT is a *P. aeruginosa* mutant (*phn*AB$^-$, *las*B$^-$ *mdo*H$^-$ and *tox*A$^-$).

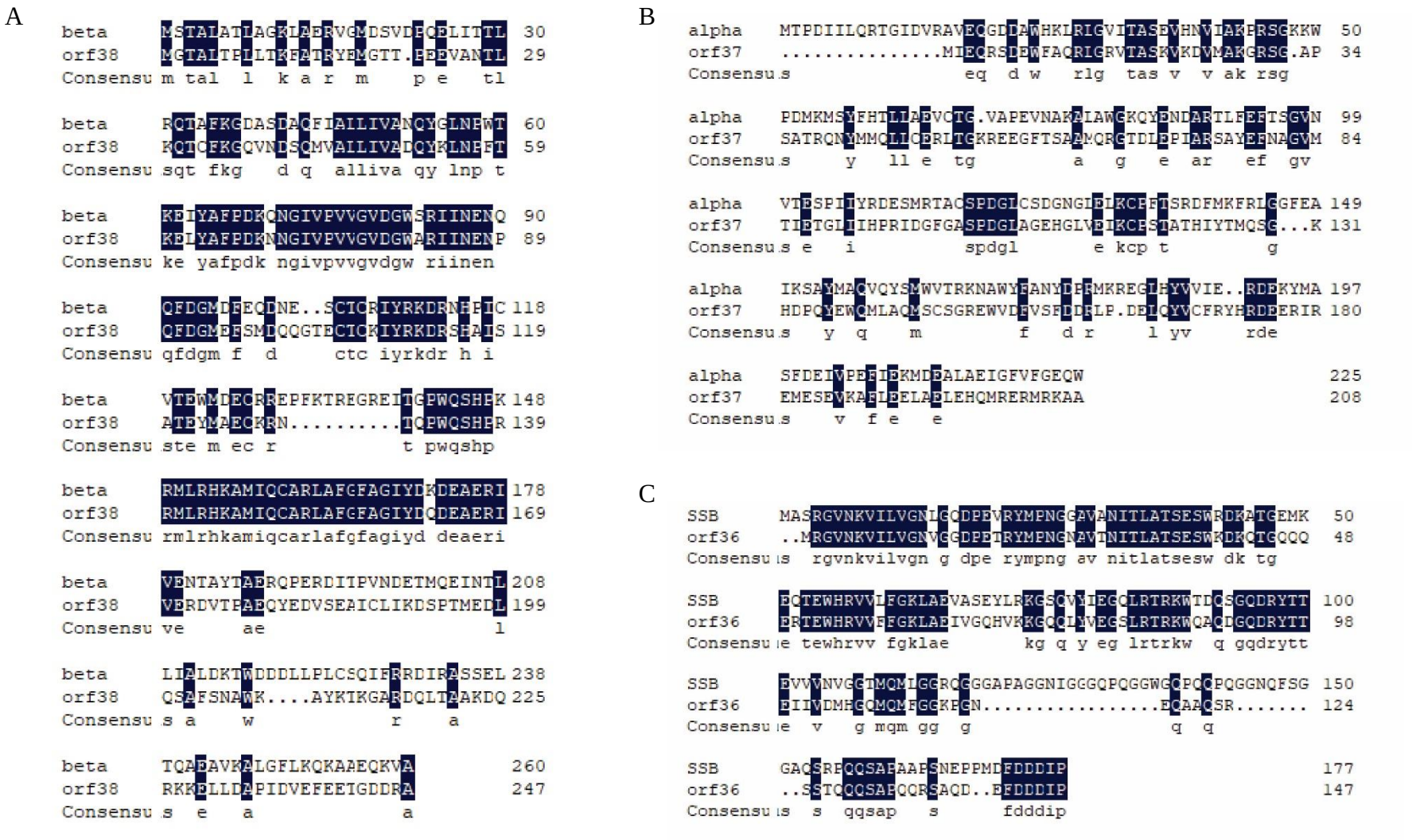

Figure S1. Protein sequence alignments between Redβ (beta) and orf38(**A**), Redα (alpha) and orf37 (**B**), and single-strand DNA-binding protein (SSB) and orf36 (**C**). Conserved sequences are shaded in black, Related to Figure 1.

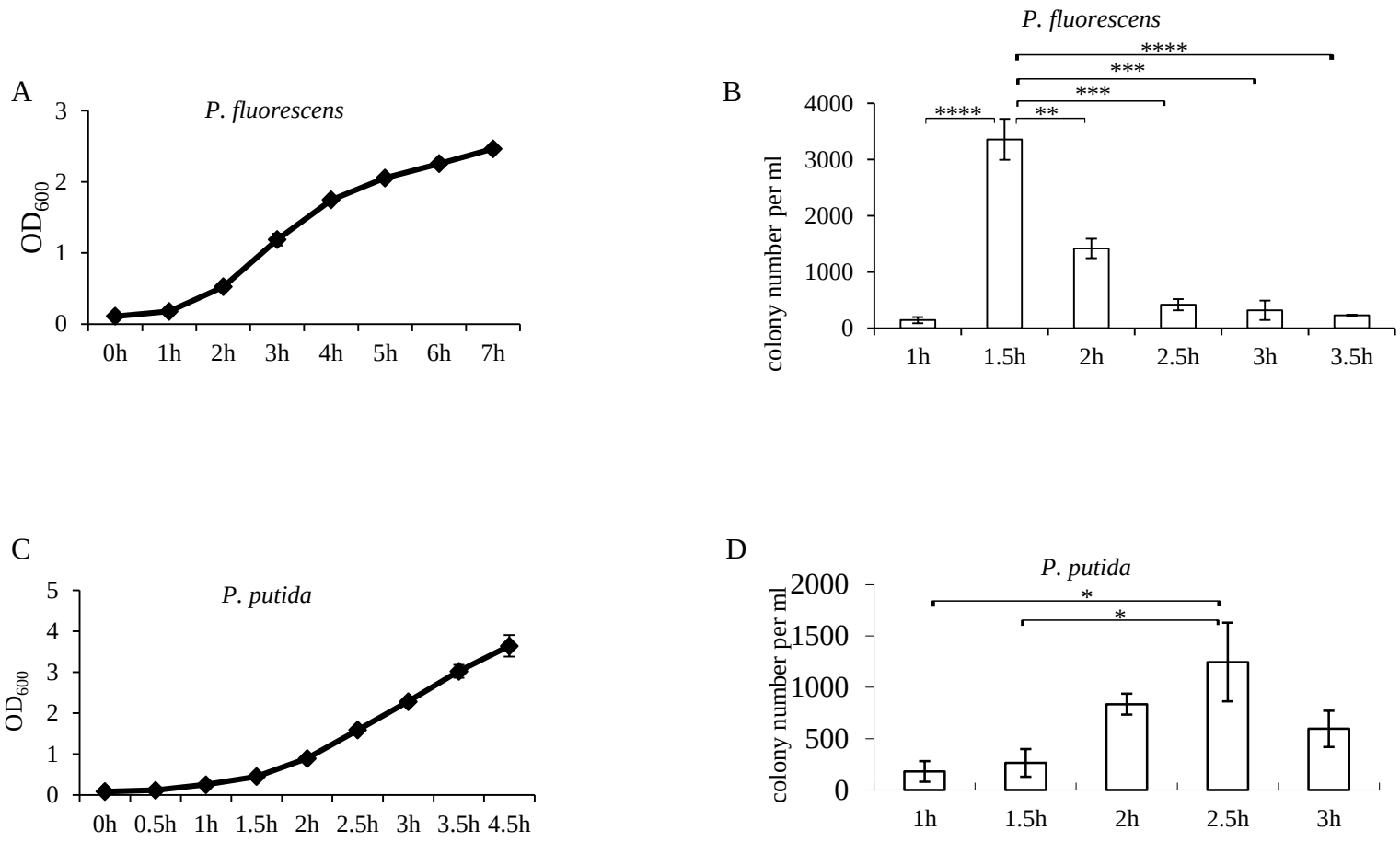

Figure S2. Optimization of transformation in *Pseudomonas*, Related to Figure 2. (**A**) and (**C**) Growth curves for *P. fluorescens* and *P. putida*. The optical density at 600 nm (OD_{600}) was measured from a starting OD_{600} of 0.085. (**B**) and (**D**) Cell competence time windows for *P. fluorescens* and *P. putida*. The plasmid pBBR1-Rha-GFP-km was electroporated into *Pseudomonas*, and colonies were selected on kanamycin plates and counted. Data represent the mean ± SD from three independent experiments. The statistical analysis used is Student's *t* test. *p<0.05, **p<0.01, ***p<0.001, ****p<0.0001.

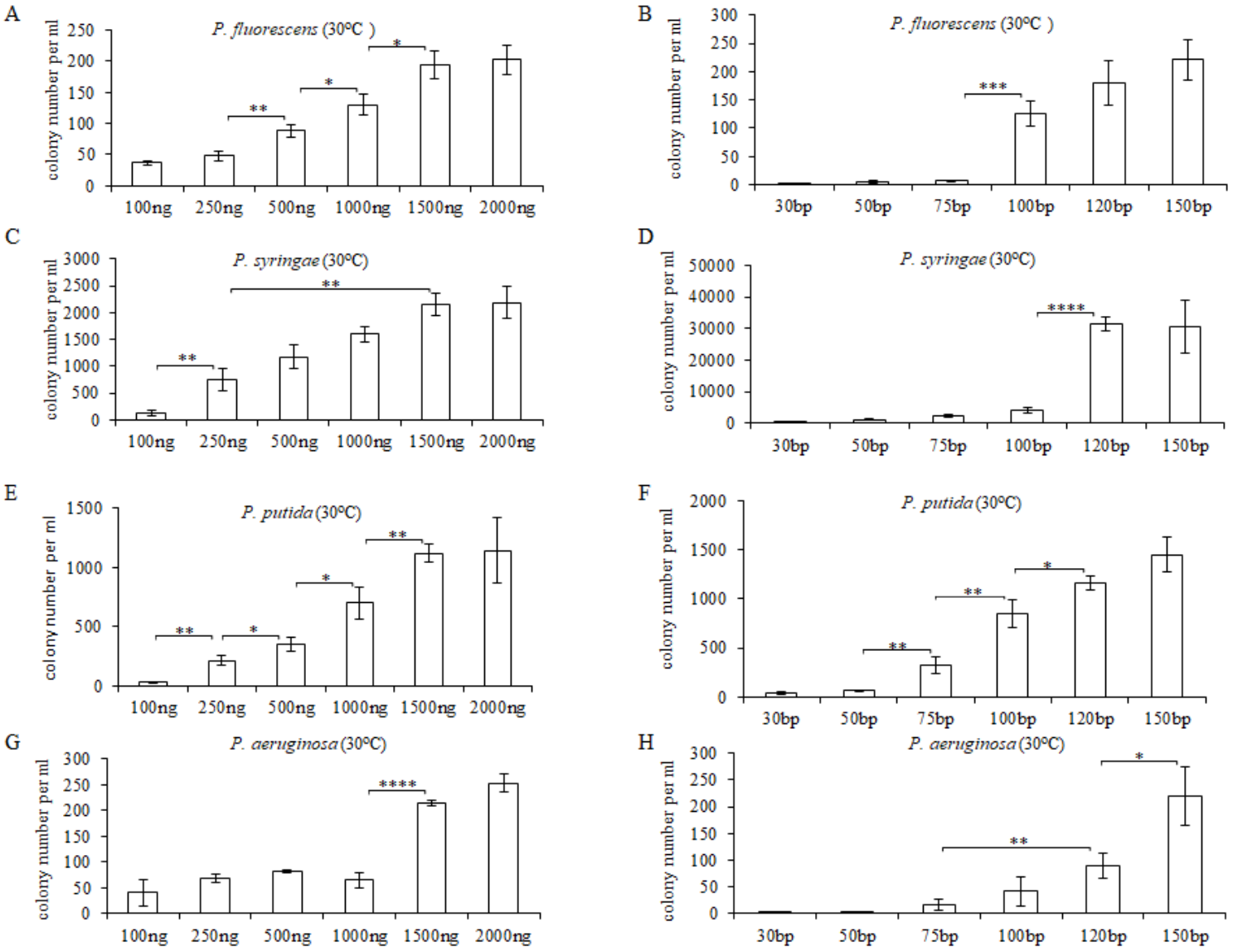

Figure S3. Optimization of recombineering in *Pseudomonas* species using the assay shown in Fig. 3A, Related to Figure 2 and 3. Titration of the DNA amount and comparison of the homology in *P. fluorescens* harbouring the RedγTE$_{Psy}$ expression plasmid (**A**) and (**B**), in *P. syringae* harbouring the BAS expression plasmid (**C**) and (**D**) and in *P. putida* harbouring the BAS expression plasmid (**E**) and (**F**), in *P. aeruginosa* harbouring the PluγTE$_{Psy}$ expression plasmid (**G**) and (**H**). Colonies were selected on gentamycin plates and counted. Data represent the mean ± SD from three independent experiments. The statistical analysis used is Student's *t* test. *p<0.05, **p<0.01, ***p<0.001, ****p<0.0001.

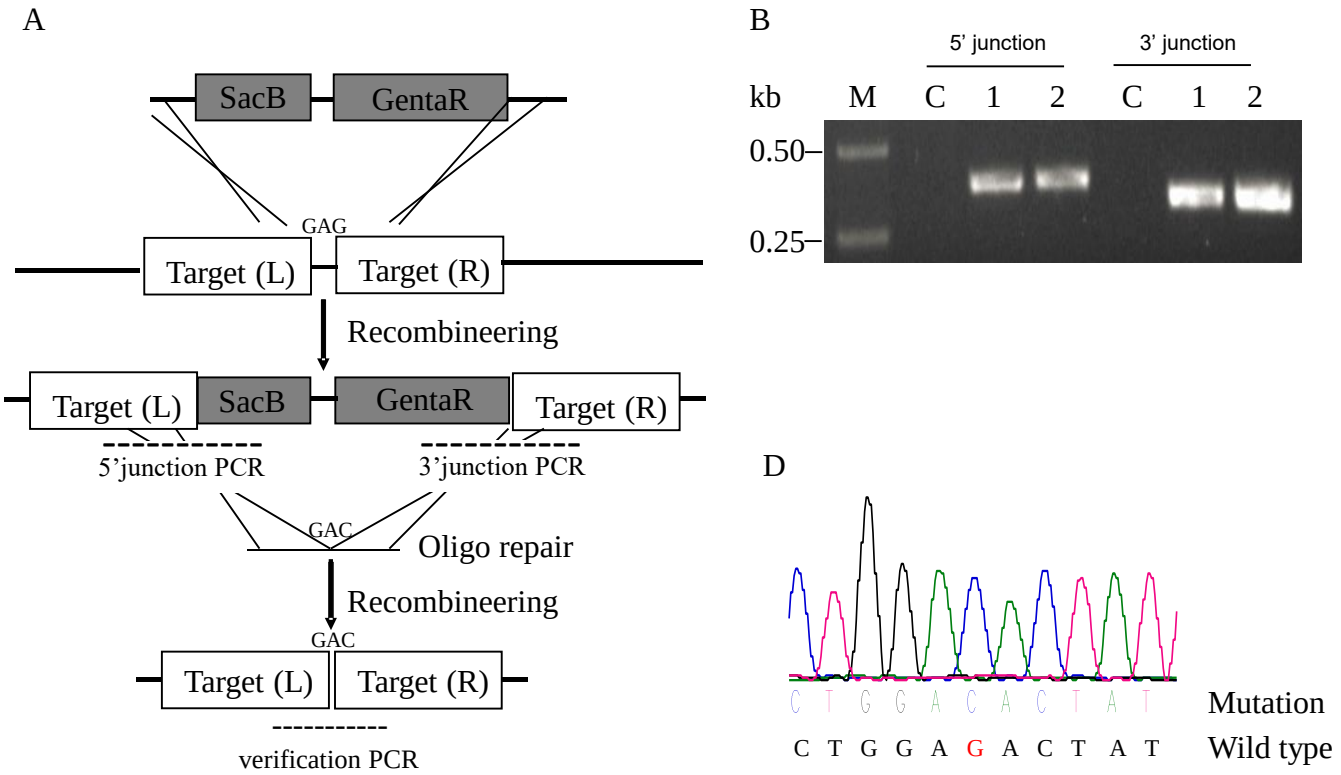

Figure S4. PCR verification of point mutations via SacB counterselection in *P. aeruginosa*, Related to Figure 5. (**A**) Diagram of seamless genome engineering in *P. aeruginosa* and schematic presentation of the PCR setup for verification. (**B**) Insertion of the SacB-genta cassette into the *tox*A target. Lane C is the wild-type strain, used as a negative control. Lane M is the Takara DL5000 marker. Lane 1 and 2 are recombinants. Both clones 1 and 2 are correct. (**C**) Introduction of the point mutation via oligo repair. The three clones are correct. (**D**) Sequencing verification of the mutant.

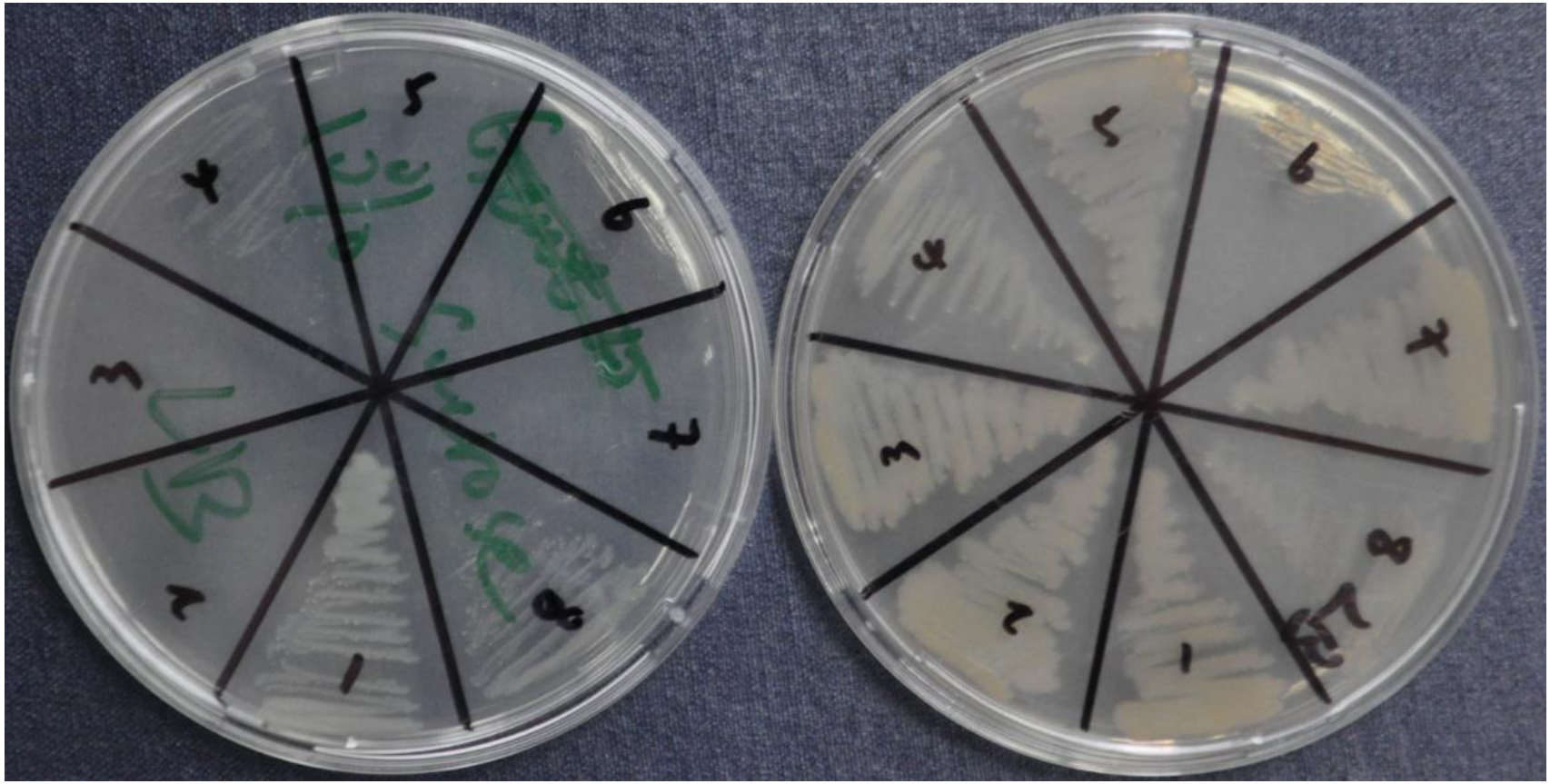

Figure S5. SacB function test on an LB plate containing 10% sucrose (left panel) and an LB plate without sucrose (right panel), Related to Figure 5. 1, Wild-type *P. aeruginosa* PAO1; 2-8, different PAO1 mutant colonies after SacB-genta cassette insertion.

Figure S6. Colony PCR verification for genome engineering of *P. syringae pv. tomato str. DC3000* and *P. fluorescens* pf5. PCRs were set up across the intact insertion, Related to Figure 5. (**A**) Insertion of the P_{genta} promoter for BGC6 expression in *P. syringae pv. tomato str. DC3000*. All three clones are correct. (**B**) Gene knockout of *ret*S in *P. fluorescens pf5*. Lane 1 is the mutant strain containing the gentaR-loxM cassette (Pf5-Δ*ret*S-genta-loxM); the clone is correct. Lanes 2 and 3 are the final mutant strain after Cre site-specific recombination (Pf5-Δ*ret*S).

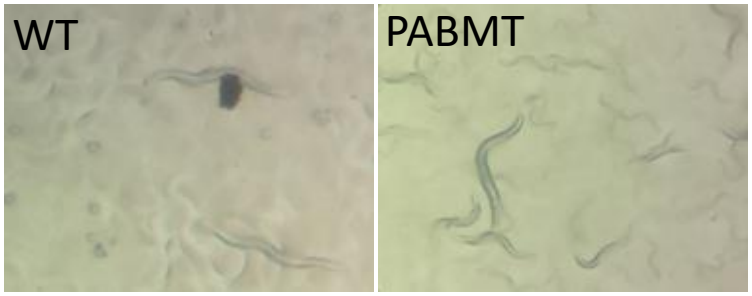

Figure S7. Toxicity test for wild-type PAO1 and the PABMT mutant ($1*10^8$ CFU) using *C. elegans*. Scale bar, 1mm, Related to Figure 5.

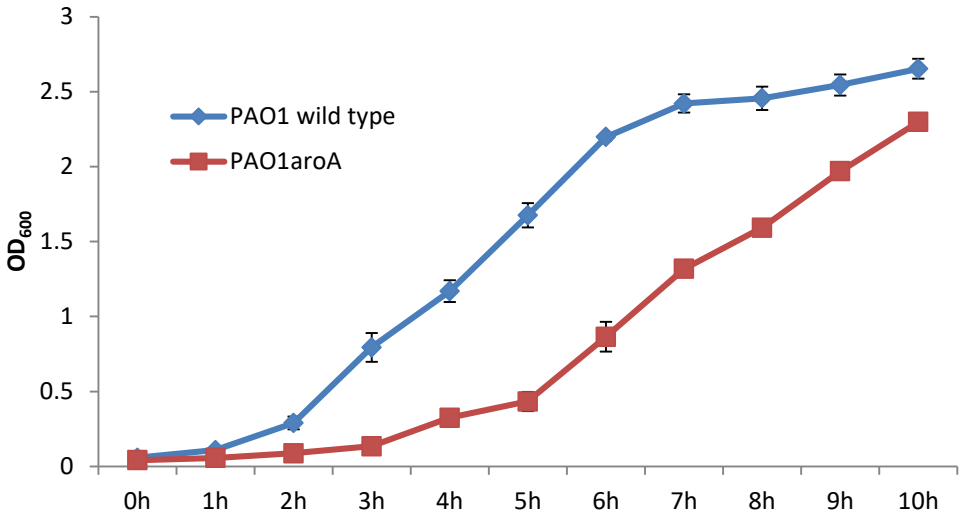

Figure S8. Growth curves of wild-type PAO1 and the PAO1*aro*A mutant, Related to Figure 6. The optical density at 600 nm (OD_{600}) was measured per hour from a starting OD_{600} of 0.085. Data represent the mean ± SD from three independent experiments.

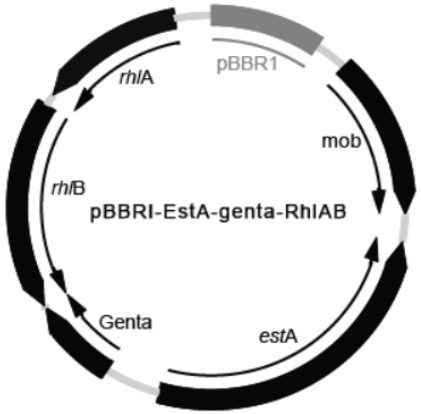

Figure S9. Diagram of the expression plasmid pBBR1-EstA-genta-RhlAB, Related to Figure 6.

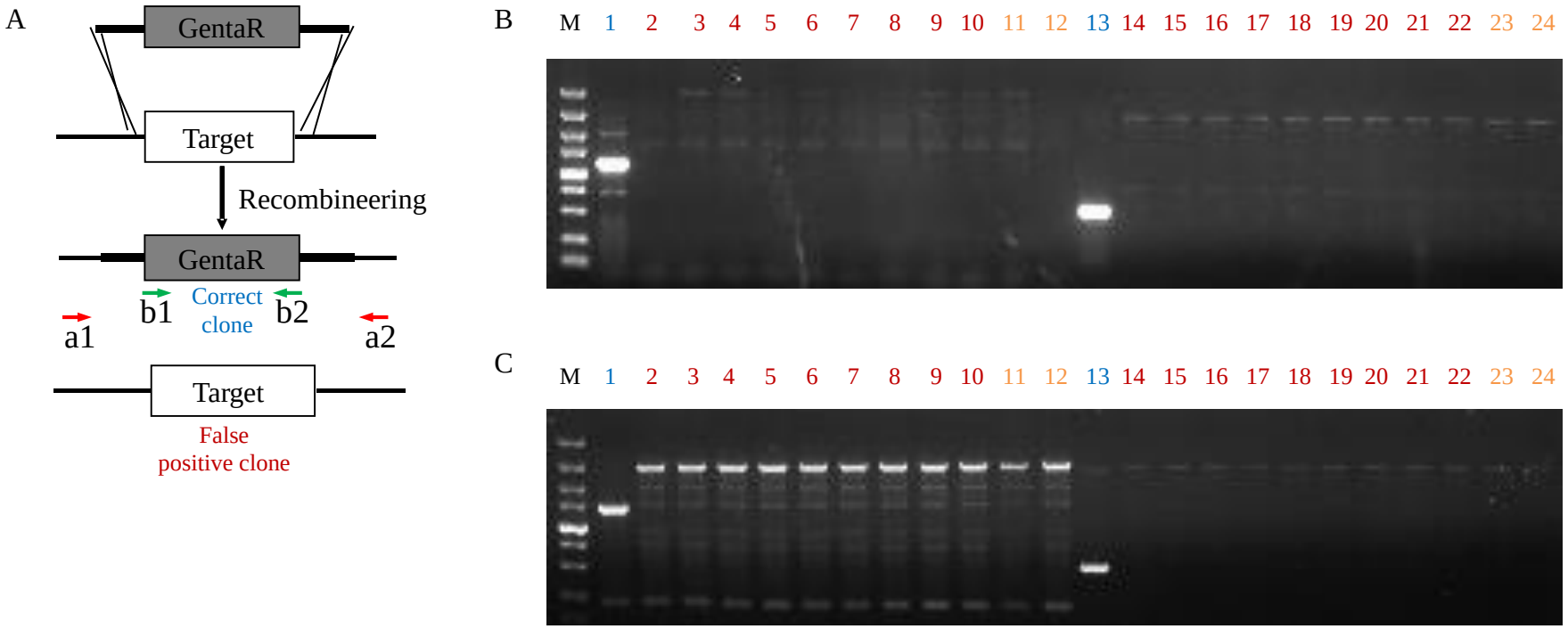

Figure S10. PCR verification of the false positive clones of *P. aeruginosa* from RedγBAS recombineering at 37°C, Related to Figure 3. (A) Diagram of the genome/plasmid engineering and schematic presentation of the PCR setup. PCR using primers (red arrows, a1/a2) across the insertion site was set up to distinguish the wild type and the recombinants. PCR using internal primer pairs (green arrows, b1/b2) binding to the gentamycin resistance gene (GentaR) was set up to check if there was any random integration of the cassette. (B) PCR verification of the plasmid engineering from the assay in Figure 3A. Lane M is the Takara DL5000 marker; Lane 1: correct clone using primers Pchk-a1/a2 (Table S3) for PCR product of 1167bp; Lane 2-10: false positive clones using primers Pchk-a1/a2 for PCR product of 4662 bp, which can not be amplified for the given polymerase and the PCR conditions; Lane 11-12: false positive clones from negative control without DNA electroporation, using primers Pchk-a1/a2 for PCR; Lane 13: correct clone using primers Gent-b1/b2 (Table S3) for PCR product of 534bp; Lane 14-22: false positive clones using primers Gent-b1/b2 for PCR product of 534bp if there was any random integration of the cassette; Lane 23-24: false positive clones from negative control without DNA electroporation, using primers Gent-b1/b2 for PCR. (C) PCR verification of the genome engineering (*mdo*H knocking out). Lane 1: correct clone using primers Hchk-a1/a2 (Table S3) for PCR product of 1299bp; Lane 2-10: false positive clones using primers Hchk-a1/a2 for PCR product of 2872 bp; Lane 11-12: false positive clones from negative control without DNA electroporation, using primers Hchk-a1/a2 for PCR; Lane 13: correct clone using primers Gent-b1/b2 for PCR product of 534bp; Lane 14-22: false positive clones using primers Gent-b1/b2 for PCR product of 534bp if there was any random integration of the cassette; Lane 23-24: false positive clones from negative control without DNA electroporation, using primers Gent-b1/b2 for PCR.

References:

Bian, X., Huang, F., Stewart, F.A., Xia, L., Zhang, Y., and Müller, R. (2012). Direct Cloning, Genetic Engineering, and Heterologous Expression of the Syringolin Biosynthetic Gene Cluster in E. coli through Red/ET Recombineering. ChemBioChem *13*, 1946-1952.

Buell, C., Joardar, V., Lindeberg, M., Selengut, J., Paulsen, I., Gwinn, M., Dodson, R., Deboy, R., Durkin, A., and Kolonay, J. (2003). The complete genome sequence of the Arabidopsis and tomato pathogen Pseudomonas syringae pv. tomato DC3000. Proc Natl Acad Sci USA *100*, 10181 - 10186.

Fu, J., Bian, X., Hu, S., Wang, H., Huang, F., Seibert, P.M., Plaza, A., Xia, L., Müller, R., Stewart, A.F.*, et al.* (2012). Full-length RecE enhances linear-linear homologous recombination and facilitates direct cloning for bioprospecting. Nat Biotechnol *30*, 440-446.

Fu, J., Teucher, M., Anastassiadis, K., Skarnes, W., Stewart, A.F. (2010). A Recombineering Pipeline to Make Conditional Targeting Constructs. Methods Enzymol *477*, 125-144.

Gross, F., Ring, M.W., Perlova, O., Fu, J., Schneider, S., Gerth, K., Kuhlmann, S., Stewart, A.F., Zhang, Y., and Muller, R. (2006). Metabolic engineering of Pseudomonas putida for methylmalonyl-CoA biosynthesis to enable complex heterologous secondary metabolite formation. Chem Biol *13*, 1253-1264.

Ni, B., Du, Z., Guo, Z., Zhang, Y.M., and Yang, R.F. (2008). Curing of four different plasmids in Yersinia pestis using plasmid incompatibility. Letters in Applied Microbiology *47*, 235-240.

Paulsen, I.T., Press, C.M., Ravel, J., Kobayashi, D.Y., Myers, G.S.A., Mavrodi, D.V., DeBoy, R.T., Seshadri, R., Ren, Q., Madupu, R.*, et al.* (2005). Complete genome sequence of the plant commensal Pseudomonas fluorescens Pf-5. Nat Biotech *23*, 873-878.

Stover, C.K., Pham, X.Q., Erwin, A.L., Mizoguchi, S.D., Warrener, P., Hickey, M.J., Brinkman, F.S.L., Hufnagle, W.O., Kowalik, D.J., Lagrou, M.*, et al.* (2000). Complete genome sequence of Pseudomonas aeruginosa PAO1, an opportunistic pathogen. Nature *406*, 959-964.